Climate Dynamics (2025) 63:353
https://doi.org/10.1007/s00382-025-07835-0

Exploring uncertainty in dynamical future changes in Sahel precipitation: the extratropical influence

Paul-Arthur Monerie[1] · **Elsa Mohino**[2] · **Marie-Pierre Moine**[3,4] · **Michela Biasutti**[5] · **Benjamin Pohl**[6] · **Juliette Mignot**[7]

Received: 5 April 2025 / Accepted: 4 August 2025

Abstract
The future changes in Sahel precipitation have significant societal implications. Yet, the projections in Sahel precipitation remain highly uncertain, partly due to strong differences across climate models in projected sea surface temperature (SST) and its effects on the atmospheric circulation. This study investigates the effects of North Atlantic and Mediterranean SST changes on future Sahel precipitation through sensitivity experiments conducted with three atmospheric models. We confirm that the warming of the North Atlantic and the Mediterranean SSTs is one of the main reasons for the discrepancies between climate model projections of Sahel precipitation. Warming in the North Atlantic and Mediterranean enhances the monsoon circulation and increases precipitation over the Sahel, primarily through dynamical effects driven by energy gradients. At the same time, we identify non-linear responses to the Atlantic warming and substantial differences between the results of each model. Thus, reducing uncertainty in Sahel precipitation projections calls for improved understanding of two issues: first, Northern Hemisphere SST changes and their representation in climate models, and second, their effects on Sahel precipitation. Additionally, we find that uncertainty in future SST changes contributes to uncertainty in high-impact weather events.

Keywords Sahel precipitation change · Uncertainty · Atmosphere-only simulations · Storylines

1 Introduction

Changes in the strength and location of the West African monsoon substantially impact the Sahel. Since the 1990s, precipitation has increased from drought conditions, but this partial 'precipitation recovery' (Nicholson 2013) has been accompanied by increased precipitation variability (Sanogo et al. 2015; Osgood et al. 2024) and risk of flooding (Ekolu et al. 2024). The precipitation recovery is associated with a decrease in anthropogenic aerosol emissions in North America and Europe (Herman et al. 2020; Marvel et al. 2020; Hirasawa et al. 2022; Monerie et al. 2022) and an increase in global greenhouse gas (GHG) concentrations (Dong and Sutton 2015; Monerie et al. 2022), through their effects on the zonal-mean cross-equatorial energy transport and regional atmospheric circulation. Regionally, over the late 20th and early twenty-first centuries, changes in GHG concentrations, anthropogenic aerosols, and internal climate variability have led to the warming of the Sea Surface Temperatures (SSTs) of the North Atlantic and the Mediterranean Sea, which promoted increased precipitation over the

✉ Paul-Arthur Monerie
pmonerie@gmail.com

1 National Centre for Atmospheric Science, Reading, UK

2 Dpto. Física de La Tierra y Astrofísica, Facultad Ciencias Físicas, Universidad Complutense de Madrid, Ciudad Universitaria, Madrid, Spain

3 CECI - Climat, Environnement, Couplages et Incertitudes, Toulouse, France

4 CERFACS, Toulouse, France

5 Lamont-Doherty Earth Observatory of Columbia University, Palisades, NY, USA

6 Centre de Recherches de Climatologie, UMR 6282 Biogéosciences, CNRS/Université de Bourgogne Franche-Comté, Dijon, France

7 LOCEAN/IPSL Sorbonne University/IRD/CNRS/MNHN, Paris, France

Published online: 05 September 2025

Sahel (Park et al. 2016). GHG concentrations are likely to continue rising towards the end of the twenty-first century (O'Neill et al. 2016), and we could expect increased precipitation across at least the central and eastern Sahel (Biasutti 2013; Monerie et al. 2020b). Yet, projections from models participating in the sixth phase of the Climate Model Intercomparison Project (CMIP6; Eyring et al. 2016) show that future changes in Sahel precipitation are uncertain (e.g., Monerie et al. 2020a, b).

CMIP-class models project a wide range of changes in precipitation over the Sahel, both in terms of intensity and patterns (Biasutti 2013; Monerie et al. 2016, 2020b, 2023; Mutton et al. 2024; Audu et al. 2024). Several models simulate a decrease in precipitation over the western Sahel and an increase over the central Sahel, resulting in a zonal contrast in precipitation change. Other models show a relatively uniform decrease or increase in precipitation (Monerie et al. 2016; Audu et al. 2024). Monerie et al. (2020a, b) investigate the sources of uncertainty in precipitation change. They show that the dynamic change in atmospheric circulation is the primary source of uncertainty in future changes in Sahel precipitation. Several authors highlight the role of future changes in SST. Guilbert et al. (2024) show that uncertainty in tropical Pacific SST leads to uncertainty in Sahel precipitation change. Park et al. (2015) show a role for cross-hemisphere temperature gradients, with models that warm the Northern Hemisphere SSTs the most producing the most substantial increase in Sahel precipitation. Park et al. (2016) build upon Park et al. (2015) and show a decisive role for the North Atlantic and Mediterranean SSTs in explaining uncertainty in precipitation change. Monerie et al. (2023) (hereafter MO23) confirm the findings of Park et al. (2016) by building a statistical model of rainfall change from North Atlantic and Euro-Mediterranean temperature changes and demonstrating the decisive contribution of the extratropical latitudes to uncertainty. Most recently, Jeong et al. (2025) also showed that CMIP6 models selected for their greater-than-average warming in the Arctic tend to wet the entire Sahel, while those selected for greater-than-average warming in the Southern Ocean tend to dry in the West, although the degree of Southern Ocean warming explains less inter-model variance than the Arctic warming.

MO23 shows that temperature changes in the North Atlantic and Euro-Mediterranean regions influence precipitation in the central Sahel, and uncertainty in their projections can explain up to 60% of the uncertainty in central Sahel precipitation change. However, MO23 does not assess the mechanisms of such influence. Here, we expand on MO23 to evaluate the sources of uncertainty in Sahel precipitation change, isolating the effects of SST variations in specific oceanic basins to replicate the range of future changes in SST gradients. We conduct a series of sensitivity experiments to test the effects of various SST change patterns in three atmosphere models, thereby accounting for model uncertainty. The study primarily describes the physical mechanisms at play. Contrasting trajectories in future Sahel precipitation are likely associated with different societally relevant impacts. We propose a first attempt to quantify the impacts on Sahel precipitation, addressing changes in heavy precipitation as well as in their contribution to seasonal mean precipitation. For this purpose, we assess changes in potential storm activity, which are linked to regional-scale temperature gradients and heavy precipitation events.

We evaluate the following scientific questions:

- Are changes in SST in the North Atlantic and Mediterranean Sea critical for understanding uncertainty in precipitation change in the Sahel, and what are the mechanisms at play?
- Are the effects of North Atlantic and Mediterranean SST changes on Sahel precipitation model-dependent?
- Can we expect significant, societally relevant impacts in West Africa?

2 Data and method

2.1 Storyline approach and CMIP6 uncertainty

We construct two storylines after MO23 using 42 CMIP6 models (Table S1), using a multiple linear regression framework to quantify the effect of different levels of warming in North Atlantic and Mediterranean SST on Sahel precipitation (MO23; Zappa and Shepherd 2017). The storylines are based on the effect of climate change, defined as the difference between the period 2060–2099 (using the SSP5-8.5 emission scenario; O'Neill et al. 2016) and the period 1960–1999 (using historical simulations) and in July–August-September (JAS). We describe the Storyline approach we employ in the Supplementary Material.

The storyline approach consists of constructing trajectories in precipitation and temperature associated with a future low and high warming in North Atlantic and Mediterranean SST, relative to the CMIP6 ensemble. We then show two plausible future trajectories of temperature change by the end of the twenty-first century. The first trajectory is based on a warming of the North Atlantic and Mediterranean Sea above the multi-model mean (Fig. 1a). The second trajectory is characterised by a weaker warming of the North Atlantic and the Mediterranean SSTs (Fig. 1b). In addition to the storyline approach, we select models that show a similar change in temperature (*i.e.*, below- and above-average changes in North Atlantic and Mediterranean SSTs)

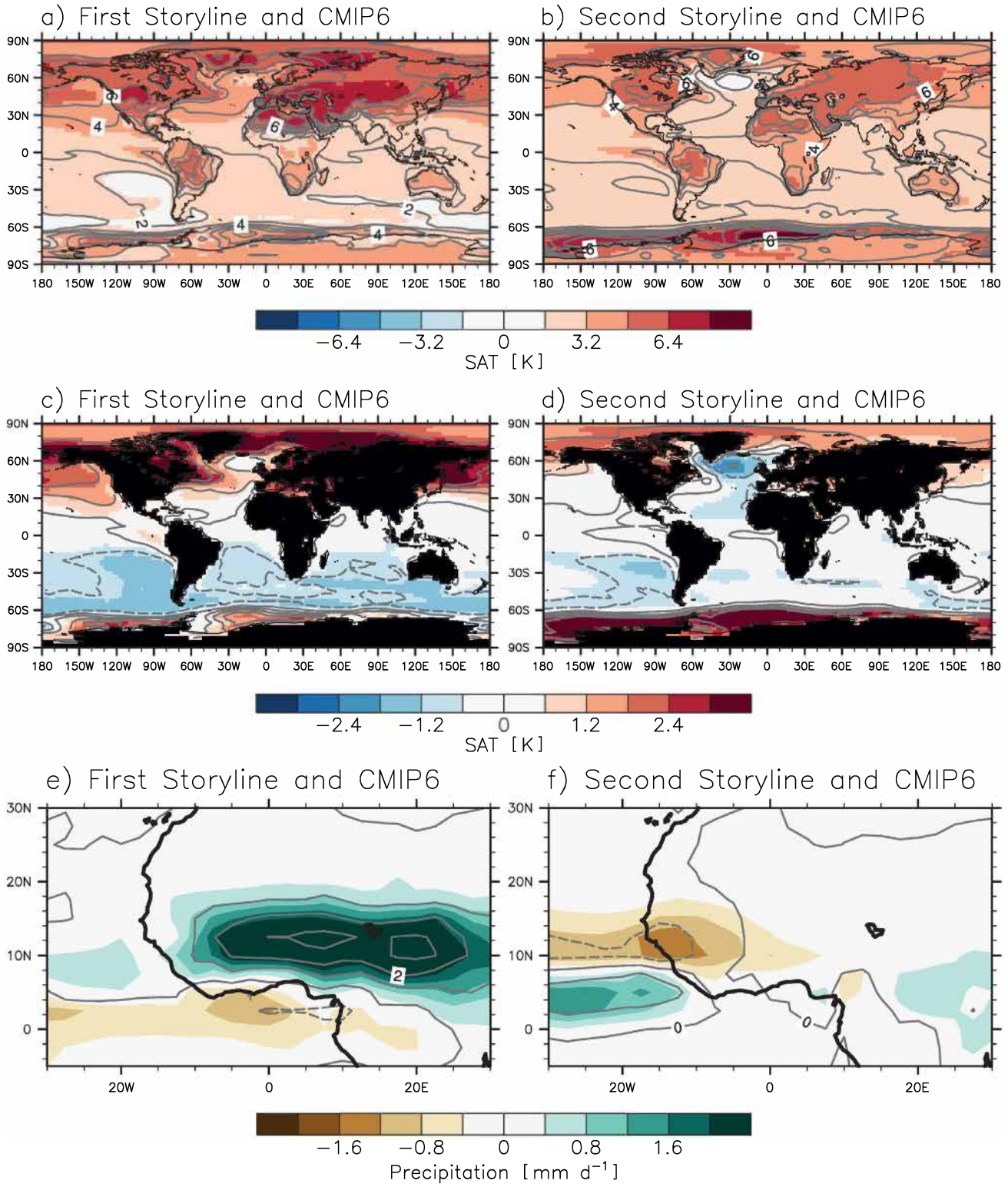

Fig. 1 Surface-air temperature changes [K] for the end of the 21st Century (period 2060–2099 minus 1960–1999) for the (**a**-**b**) two storylines. The contours show surface-air temperature change obtained for two groups of CMIP6 models that show the same behaviour in surface-air temperature change as the two storylines by the end of the twenty-first century (See text for further details; contours from −2 K to +8 K every 1 K). **c** and **d**, as in **a** and **b**, but after subtracting the global mean average from **a** and **b** (contours from −3 K to +3 K every 1 K) and considering the ocean grid points only. **e** and **f**, as in **a** and **b** but for changes in precipitation [mm d^{-1}] (contours in −2 mm d^{-1} to +3 mm d^{-1} every 1 mm d^{-1})

(Table S2) and show that the future storyline trajectories can be found in specific members of the CMIP6 ensemble (compare the shading to contours in Fig. 1). The group of models showing the lowest changes in the North Atlantic and Mediterranean SSTs comprises 14 models (CAS-ESM2-0, CESM2, CESM2-WACCM, CNRM−ESM2-1, FGOALS-G3, FIO-ESM2-0, GFDL-ESM4, GISS-E2-1-H, HADGEM3-GC31, IITM−ESM, KACE-1-0-G, MCM−UA, MRI-ESM2-0, TAIESM1) (Swapna et al. 2018; Kuhlbrodt et al. 2018; Yukimoto et al. 2019; Li et al. 2019, 2020; Stouffer 2019; Séférian et al. 2019; Danabasoglu et al. 2020; Lee et al. 2020; Kelley et al. 2020; Dunne et al. 2020; Dong et al. 2021; Wang et al. 2021). The group of models showing the highest changes in the North Atlantic and Mediterranean SSTs comprises 9 models (ACCESS-ESM1-5, CMCC-CM2-SR5, EC-EARTH3-VEG, E3SM−1-1, GFDL-CM4, INM−CM5-0, MIROC-ES2L, MIROC6, NESM3) (Volodin et al. 2017; Cao et al. 2018; Cherchi et al. 2019; Golaz et al. 2019; Tatebe et al. 2019; Held et al. 2019; Hajima et al. 2020; Wyser et al. 2020; Ziehn et al. 2020), following MO23.

Monerie et al. (2020a, b) show that the primary source of uncertainty lies in the differences between models in simulating the shift in atmospheric circulation. Here, we follow MO23 and Guilbert et al. (2024) in assuming that SST patterns and gradients are crucial for understanding uncertainty in the future change of the atmospheric circulation over West Africa. In other words, we focus on the pattern effect and do not assess the effect of a uniform increase in SST. We emphasise the changes in temperature gradients by removing the change in the global mean surface air temperature, considering only ocean grid points. In this light, the first storyline appears as a quite zonally uniform pattern best described as an interhemispheric temperature gradient (Fig. 1c). The second storyline is characterised by North Atlantic SST cooling relative to the global mean (Fig. 1d) with a horseshoe anomaly reminiscent of a negative phase of the Atlantic Multidecadal Variability (Knight et al. 2005), which is compatible with a weakening of the Atlantic Meridional Overturning Circulation (Caesar et al. 2018; Liu et al. 2020).

The first storyline is associated with increased precipitation over the Sahel, characterised by a meridional anomaly dipole extending over the ocean. This indicates a strengthening and northward shift of the monsoon-ITCZ system (Fig. 1e). The other storyline is associated with a southward shift of precipitation over the Atlantic Ocean and a decrease in precipitation over the western Sahel (Fig. 1f). The patterns in precipitation, as obtained with the storyline approach, are also found in the two subsets of the CMIP6 ensemble that match each trajectory (Fig. 1e and f; contours). We show in Fig. S1 that both approaches (storyline and group clustering) are successful in capturing uncertainty in Sahel precipitation across the entire CMIP6 ensemble. In the reminder of MO23, the CMIP6 uncertainty is defined as the difference in the mean of the two subsets of CMIP6 models.

2.2 The atmosphere models

We use three atmosphere models to evaluate the effects of the changes in SSTs associated with the two storylines we described in Sect. 2.1. The three atmosphere models are described below, and the experiments we performed are outlined in Sect. 2.3.

2.2.1 GA7

We use the Unified Model Global Atmosphere 7.0 (GA7, Walters et al. 2019) from the UK Met Office. GA7 has a N216 resolution (0.83° longitude and 0.55° latitude) and is a high-top model (the top level is the 0.030 hPa pressure level). A more in-depth description of the UM GA7 atmosphere model is given by Walters et al. (2019). GA7 is the atmospheric component of HadGEM−GC31, one of the UK Met Office models that contribute to CMIP6. The Joint UK Land Environment Simulator (JULES; Best et al. 2011) simulates the land surface properties.

2.2.2 LMDZ

We use the LMDZOR version 6.1.10 model (hereafter referred to as LMDZ). It is the atmospheric component of the IPSL-CM6-LR model used in CMIP6 and developed at Institut Pierre-Simon Laplace (IPSL). LMDZ uses a regular grid with 144 × 142 points, corresponding to 2.5° × 1.27° in longitude and latitude, respectively. It has 79 levels in the vertical, extending up to 80 km in height (high-top model). The land surface properties are simulated using ORCHIDEE version 2.0 (Krinner et al. 2005; Boucher et al. 2020). A detailed description of the model is provided by Hourdin et al. (2020).

2.2.3 ARPEGE

ARPEGE-Climat 6.3 (hereafter referred to as ARPEGE) is an atmosphere model conjointly developed by CNRM (Centre National de la Recherche Météorologique) and CERFACS (Centre Européen de Recherche et de Formations Avancées en Calcul Scientifique) and used for the CMIP6 version of the CNRM/CERFACS ocean–atmosphere coupled model (CNRM−CM6). ARPEGE is a high-top model with 91 vertical levels (up to 0.01 hPa) and a horizontal resolution of 1.4° × 1.4°. SURFEX (SURFace EXternalisée; Masson et al. 2013) allows land–atmosphere coupling, generating the

Table 1 Name of the experiments, number of ensemble members and length of the integrations

Experiment	Characteristics	GA7	LMDZ	ARPEGE
CTRL	Fixed SST (1981–2012) and GHG concentration (1980–2020)	10 ensemble members; 10 years	5 ensemble members; 10 years	10 ensemble members; 10 years
GLOBAL+	As in CTRL but with an imposed GLOBAL+ SST pattern (Fig. 2a)	5 ensemble members; 10 years		
GLOBAL−	As in CTRL but with an imposed GLOBAL− SST pattern (Fig. 2b)	5 ensemble members; 10 years		
NHM+	As in CTRL but with an imposed NHM+ SST pattern (Fig. 2c)	9 ensemble members; 10 years		
NHM−	As in CTRL but with an imposed NHM− SST pattern (Fig. 2d)	9 ensemble members; 10 years		
A+M+	As in CTRL but with an imposed A+M+ SST pattern (Fig. 2e)	10 ensemble members; 10 years	5 ensemble members; 10 years	10 ensemble members; 10 years
A−M−	As in CTRL but with an imposed A−M− SST pattern (Fig. 2f)	10 ensemble members; 10 years	5 ensemble members; 10 years	10 ensemble members; 10 years
A+	As in CTRL but with an imposed A+ SST pattern (Fig. 2g)	10 ensemble members; 10 years	5 ensemble members; 10 years	
A−	As in CTRL but with an imposed A− SST pattern (Fig. 2h)	10 ensemble members; 10 years	5 ensemble members; 10 years	
M+	As in CTRL but with an imposed M+ SST pattern (Fig. 2i)	10 ensemble members; 10 years	5 ensemble members; 10 years	
M−	As in CTRL but with an imposed M− SST pattern (Fig. 2j)	10 ensemble members; 10 years	5 ensemble members; 10 years	
A-extended to the tropics	As in A-but with an imposed SST pattern that extends to the South Atlantic Ocean	10 ensemble members; 10 years		

surface fluxes. A detailed description of ARPEGE is provided by Roehrig et al. (2020).

2.3 The sensitivity experiments

We perform atmosphere-only (AGCM–Atmospheric General Circulation Models) simulations where the SST anomalies are imposed on a reference climatology. This allows the exploration of the response of different AGCMs to the exact same SST patterns and to isolate the influence of the atmospheric response to SST changes on precipitation. Furthermore, we anticipated the need to conduct numerous simulations to extract a robust signal (for example, we have 1080 years of simulations with GA7). The control simulations are forced by seasonally varying climatological SST and sea ice concentration and volume, averaged over 1981–2012, using the Reynolds SST (Reynolds et al. 2007), and using the same exact annual cycle for each simulated year. We impose the exact same anomalies in the three models. The GHG and aerosol concentrations are fixed to the 1980–2020 time average.

We assess the effects of different SST anomaly patterns by forcing the three different atmosphere models with the anomalies obtained in MO23 (Fig. 1c and d) but using the SST outputs to compute the storylines. Each simulation lasts 10 years and has between 5 and 10 ensemble members, differing only in their initial conditions (using a different day to initialise the atmosphere model) (Table 1).

A set of simulations is performed using the global SST patterns, assessing the effects of temperature changes over the extratropics and the tropics (Fig. 2a and b; hereafter referred to as GLOBAL+and GLOBAL−). Other simulations evaluate the effect of changes in the Northern Hemisphere SST only (Fig. 2c and d; NHM+and NHM−), the North Atlantic and the Mediterranean Sea together (Fig. 2e and f; A+M+and A−M−), and separately (Fig. 2g–j; A+, A−, M+, and M−). See a description of the simulations in Table 1. Ideally, we would perform all simulations with each of the three atmosphere models to assess model uncertainty in the effects of SST anomalies on Sahel precipitation. However, we only performed a subset of the simulations with LMDZ and ARPEGE because of a lack of computer resources. We conduct the control simulation (CTRL) alongside the A+M+and A−M− experiments using the three models because the two former SST patterns have been shown to best characterise uncertainty in Sahel precipitation change in MO23 (Fig. S1). The simulations are used to show the effects of each SST anomaly pattern (Table 2). We also performed A+, A−, M+, and M− with LMDZ.

We assess the ability of the climate models to simulate seasonal mean (JAS) precipitation over West Africa under climatological control conditions (Fig. S2). All models

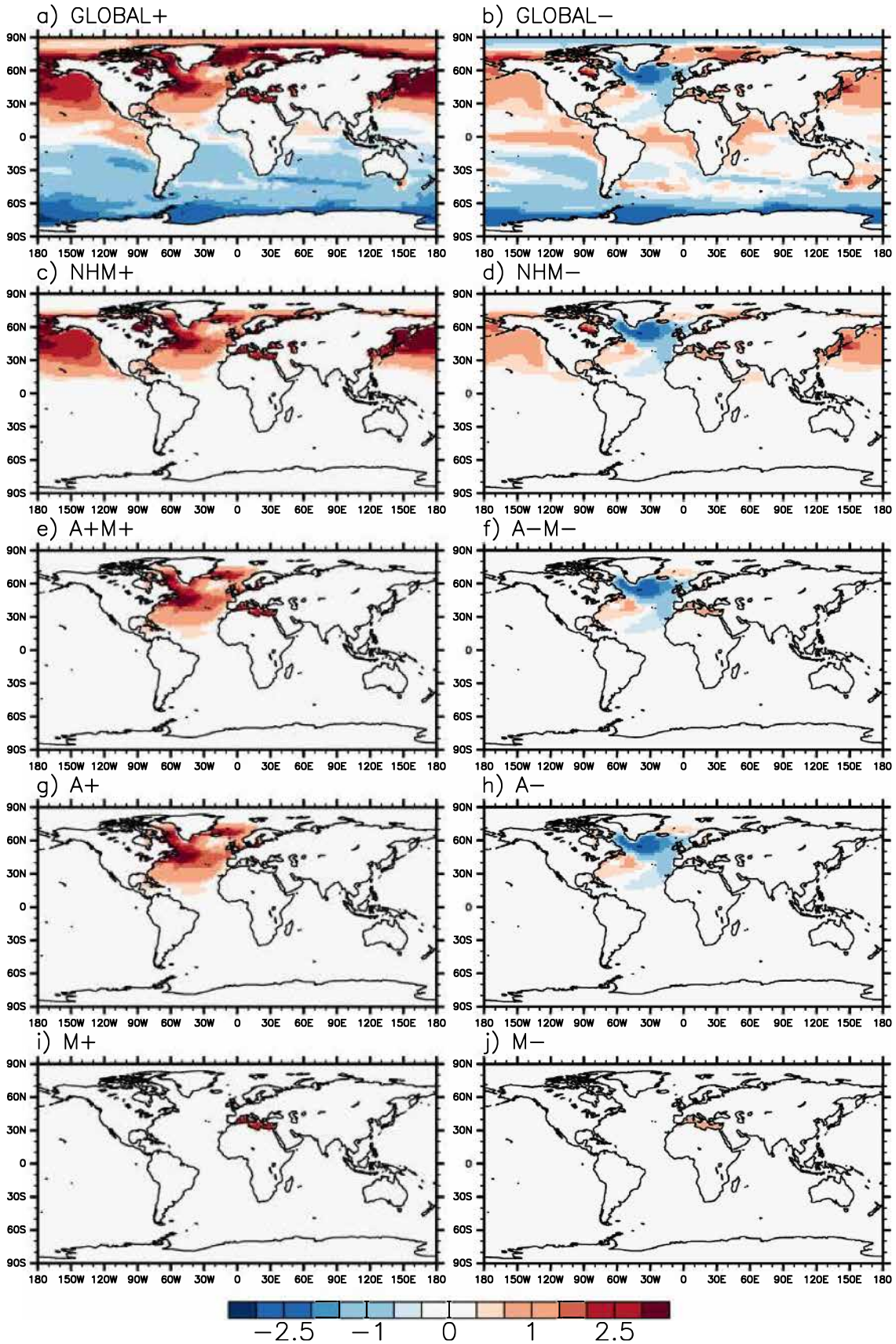

Fig. 2 Anomalies in sea surface temperature [K] in each of the sensitivity experiments: **a** GLOBAL+; **b** GLOBAL−; **c** NHM+; **d** NHM−; **e** A+M+; **f** A−M−; **g** A+; **h** A−; **i** M+; and **j** M−

Table 2 Summary of the different impacts on the Sahel precipitation highlighted by the simulations presented in Table 1 and described in Sect. 2.2

Name	Simulation differences	Highlighted impacts
GLOBAL+, GLOBAL−, NHM+, NHM−, A+M+; A−M−; A+; A−; M+; M−	Difference between [A+M+], [A−M−], [A+], [A−], [M+], [M−], and [CTRL], respectively	The impacts of each experiment are listed in Table 1 relative to the CTRL simulation
GL	[GLOBAL+]–[GLOBAL−]	The impact of two contrasted projections in global SST
NHM	[NHM+]–[−NHM−]	The impact of two contrasted projections in the Northern Hemisphere SST
AM	[A+M+]–[A−M−]	The impact of two contrasted projections in the North Atlantic and the Mediterranean SST
A	[A+]–[A−]	The impact of two contrasted projections in the North Atlantic SST
M	[M+]–[M−]	The impact of two contrasted projections in the Mediterranean SST

underestimate precipitation over the Sahel, exhibiting a dry bias (Fig. S3) that was shown to be systematic in the CMIP6 ensemble (*e.g.*, Monerie et al. 2020a, b). The bias is of similar magnitude for all three models in the Sahel region (Fig. S3).

2.4 Decomposing changes in precipitation

We decompose precipitation anomalies into terms that document dynamic and thermodynamic changes, following Chadwick et al. (2016).

The assumption is that precipitation anomalies can be approximated by

$$P = M^* q, \tag{1}$$

where P is precipitation, M^* is a proxy for convective mass flux from the boundary layer to the free troposphere (M^* = p/q), and q is the near-surface specific humidity (at ~ 2 m), following Held and Soden (2006). We then obtain that

$$\Delta P = \Delta \left(M^* q \right), \tag{2}$$

with Δ indicating the difference between two sets of simulations (*e.g.*, between A+M+ and A−M− when quantifying the effects of the change in North Atlantic and Mediterranean SSTs; see the pair of simulations in Table 2). An increase in precipitation can be due to an increase in specific humidity (thermodynamic) and to an increase in how the atmospheric circulation pumps up moisture to allow convection (dynamic). Precipitation change is decomposed as follows (Chadwick et al. 2016):

$$\Delta P = M^* \Delta q + q \Delta M^* + \Delta q \Delta M^*, \tag{3}$$

This expression can be written:

$$\Delta P = \Delta P_{therm} + \Delta P_{dyn} + \Delta P_{cross}, \tag{4}$$

with ΔP_{therm} the change in precipitation that is due to the change in specific humidity (the thermodynamic term), ΔP_{dyn} the change in precipitation that is due to the change of the atmospheric circulation (the dynamic term), and ΔP_{cross} is the non-linear cross term, which is associated with changes in both the thermodynamic and the dynamic terms.

2.5 Moist static energy

The dynamics of the West African Monsoon are controlled by meridional gradients in moist static energy (MSE) through changes in latent, sensible, and geopotential energy between the hot Saharan desert and the humid Guinean zone (Eltahir and Gong 1996; Fontaine and Philippon 2000; Gaetani et al. 2017). Precipitation is directly linked to MSE, a quantity approximately conserved in moist convection, as lower tropospheric enthalpy and latent energy transform into geopotential energy in the upper levels.

MSE is defined as

$$MSE = gz + c_p T + L_v q, \tag{5}$$

where gz is the geopotential energy, with g the gravitational acceleration and z the geopotential height. $c_p T$ is the enthalpy, with c_p the specific heat of dry air at constant pressure, and T is the temperature. $L_v q$ is the latent energy associated with evaporation and condensation of water, with L_v the latent heat of evaporation and q the specific humidity.

We account for the meridional gradient in MSE (hereafter referred to as ∇MSE) by integrating MSE between the surface to the top of the troposphere (10 hPa) and by computing a bulk meridional gradient (differences between 20°N–30°N and 5°N–15°N, averaged over longitudes 10°W–10°E following Gaetani et al. (2017).

2.6 Heavy precipitation

We quantify the effect of the different SST anomaly patterns on the uncertainty in projections of intense precipitation events. We use the R10mm index, following the Expert Team on Climate Change Detection and Indices (ETCCDI) (Sillmann et al. 2013). R10mm documents the days we register precipitation daily of at least 10 mm, which can also be characterised as heavy precipitation events. In GA7, ARPEGE, and LMDZ, there are generally ~ 0–4 heavy events over the Sahel, up to 10 along the coast near the Gulf of Guinea, and up to 20 events over the high orography (e.g., FoutA−Djallon in Guinea, Cameroon high) each month and in summer (not shown). We also assessed the effects of the very heavy precipitation events (of at least 20 mm d^{-1}). In addition, we quantify the effect of changes in extremes on seasonal mean precipitation.

2.7 Meridional temperature gradient and storm activity

We describe how distinct pathways in SST change can affect precipitation extremes across the Sahel, connecting the latter to the changes in atmospheric circulation and temperature gradients that support storm activity. Observational studies suggest that the frequency of storms has increased over the recent decades in the Sahel (Taylor et al. 2017). The storm activity associated with large mesoscale convective systems cannot be directly assessed by the models we use due to their inadequate vertical and horizontal resolution and parameterisation of convection. We use the large-scale meridional lower-tropospheric temperature gradient (hereafter referred to as ∇T) as a proxy for mesoscale systems development in the CMIP-class model (Rowell et al. 2021). An increase in ∇T is related to increased vertical wind shear and a strengthening of the storm activity. We expect changes in precipitation to affect the temperature gradients through subsequent changes in soil moisture and evaporation. However, Rowell et al. (2021) show that anomalies in ∇T are primarily related to a warming-advection-circulation feedback, while anomalies in evaporation weakly affect ∇T. Therefore, we expect ∇T not to be dramatically impacted by the changes in precipitation, but to be associated with anomalies in atmospheric circulation across the Sahel.

∇T is estimated by the linear regression slope between the zonal mean 850 hPa temperature and latitude after Rowell et al. (2021). The tropospheric temperature zonal mean is computed from 10°W to 10°E and for each degree of latitude between 10 and 30°N to account for the northward shift of the monsoon system.

3 Results

3.1 Explaining uncertainty in Sahel precipitation

We assess the effects of the SST anomaly patterns on Sahel precipitation projection uncertainty (Table 1) and compare them with the range of outcomes obtained from the CMIP6 models and the storyline approach. Sahel precipitation is defined as the area average between 10°W and 20°E and 10°N and 20°N, in July, August, and September (JAS).

The CMIP6 uncertainty (defined as the difference in the mean of the two subsets of CMIP6 models; See Sect. 2.1 and Table S2) of the dynamic change in precipitation (ΔP_{dyn}) is ~ 0.9 mm d^{-1}, around twice as big as the sum of the thermodynamic and cross non-linear terms (ΔP_{therm} and ΔP_{cross}) (Figs. 3a and S4). The uncertainty in simulating the dynamic change in precipitation (ΔP_{dyn}) is thus the main source of uncertainty in Sahel precipitation change (Monerie et al. 2020b). We assess how the AGCM responses to contrasting SST compares to the CMIP6 uncertainty. Uncertainty in projected SST (i.e., [Global+]–[GLOBAL−]) is associated with a difference in ΔP_{dyn} of ~ 0.8 mm d^{-1} in GA7 (Fig. 3a), comparable to the CMIP6 uncertainty and suggesting that the GA7 simulations allow us to assess the CMIP6 uncertainty sources in ΔP_{dyn} (Fig. 3a).

We note that the change in precipitation, ΔP_{therm} and ΔP_{cross}, are smaller in the GA7 simulations than for the CMIP6 ensemble (for the change in global SST, as shown by the difference between GLOBAL+ and GLOBAL−) (Fig. 3a). This is to be expected given that the global mean temperature change is designed to be close to zero in GLOBAL+ and GLOBAL− (because the global mean SST was subtracted; Fig. 2a and b), while there are differences in the changes in global mean temperature among the CMIP6 simulations. These differences in global mean temperature lead through the Clausius-Clapeyron relation to changes in moisture, which strongly control the precipitation thermodynamic response, and which is thus moderate in GLOBAL+ and GLOBAL−.

We show that the effect of global SST change on Sahel precipitation uncertainty is primarily (72%) contributed by the Northern Hemisphere temperature change (Fig. 3a and b; GA7) (*i.e.*, the effect of GL -as defined in Table 2- is of ~ 1.02 mm d^{-1} and the change of NHM is 0.74 mm d^{-1}), in agreement with Park et al. (2016). More specifically, we show that the change in North Atlantic

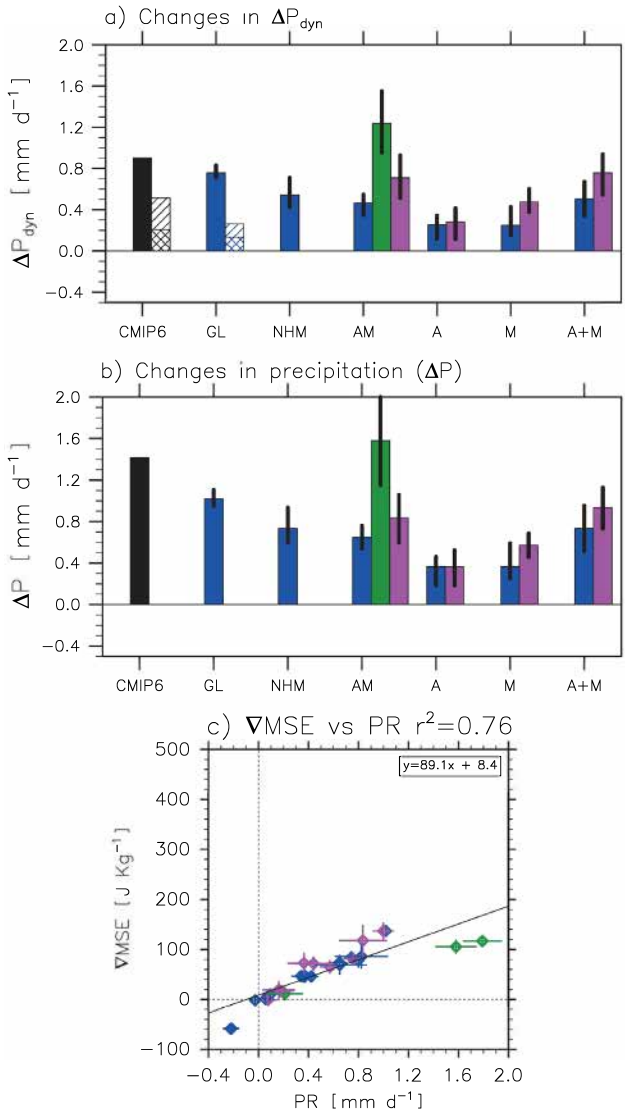

Fig. 3 **a** Uncertainty range in Sahel precipitation [10°W–20°E; 10–20°N] that is associated with the change in atmospheric circulation (ΔP_{dyn}) [mm d^{-1}] in JAS within the CMIP6 ensemble (CMIP6), due to the global SST anomaly pattern (GL, i.e., [GLOBAL+]–[GLOBAL−]), to the SST anomaly SST pattern over the Northern Hemisphere (NHM, i.e., [NHM+]–[NHM−]), to the change in North Atlantic and Mediterranean SST (AM, i.e., [A+M+]–[A−M−]), to the change in North Atlantic SST (A, i.e., [A+]–[A−]), Mediterranean SST (M, i.e., [M+]–[M−]). [A+M] shows the sum of the effects of the North Atlantic (A) and Mediterranean (M) SSTs. The results of GA7 are shown with a blue bar, ARPEGE with a green bar and LMDZ with a magenta bar. The vertical line denotes the uncertainty, that is, the range between the minimum and maximum values in the change in Sahel precipitation as obtained for CMIP6 and each pair of experiments. **b** as in **a** but for the total precipitation change. In **a** and **b**, all anomalies are statistically significant according to a Student's t-test at the 95% confidence level. In **a** diagonal hatching and diagonal cross-hatching show the change in precipitation that is due to ΔP_{cross} and ΔP_{therm}, respectively. **c** changes in meridional gradient in MSE [J Kg^{-1}] (∇MSE) in function of the change in precipitation [mm d^{-1}] for each pair of experiments. In **c**, the vertical and horizontal lines denote the uncertainty in changes in the meridional gradient in MSE and precipitation, respectively, as estimated by two times the standard error. In **c**, we show the difference between all pairs of experiments

and Mediterranean SST (~0.65 mm d^{-1}) strongly affects Sahel precipitation uncertainty (88% of the effect of the Northern hemisphere temperature change and 64% of the effect of the global pattern).

We performed the A+M+ and A−M− simulations with GA7, LMDZ, and ARPEGE. In all models, we show that the increase in North Atlantic and Mediterranean SSTs (A+M+) is associated with increased precipitation over the Sahel, showing consistency in the effects of extratropical SST change on Sahel precipitation change. Nevertheless, model uncertainty is substantial, with considerable differences in the magnitude of changes in Sahel precipitation among the models. ARPEGE simulates a change in precipitation that is ~2.5 times greater than in GA7 and ~1.9 times greater than in LMDZ. These differences persist when the anomalies are expressed as a percentage of the climatology, thus confirming a stronger sensitivity in ARPEGE than in LMDZ and GA7 to the effects of North Atlantic and Mediterranean SSTs on precipitation (Fig. S5). In addition to the uncertainty in SST patterns and magnitude, understanding how models simulate the effect of SST on Sahel precipitation is crucial for understanding the future changes in Sahel precipitation.

Intriguingly, both GA7 and LMDZ simulate similar responses to the change in North Atlantic and Mediterranean SST (Fig. 3a and b) and the effects of the two basins sum up linearly (*i.e.*, [A]+[M]~[AM]). This confirms the results of MO23 but contradicts the results of Park et al. (2016) with ECHAM6, which show a strong predominance of the Mediterranean SST for future changes in Sahel precipitation.

We assess the local manifestation of the change in the energy budget by assessing the change in the meridional gradients in column-integrated MSE (Sect. 2.5; ∇MSE). In all our AGCM pairs of simulations, the uncertain change in SST (magnitude and pattern) is associated with an extensive range of changes in ∇MSE ($r^2 = 0.76$) (Fig. 3c). A strengthening of the meridional MSE gradient is associated with an increase in Sahel precipitation, with MSE increasing mostly over the northern edge of the Sahel in all models (Fig. S6). Such gradient was shown to affect Sahel precipitation through energy redistribution and energy gradients (e.g., Gaetani et al. 2017), and indeed we find that the change in Sahel precipitation is particularly sensitive to the MSE of the lower troposphere (surface to 700 hPa; $r^2 = 0.74$; not shown). In addition to the ∇MSE we computed the meridional gradients in dry static energy (∇DSE, which is the sum of the enthalpy and geopotential energy) and found a relatively low relationship between the change in precipitation and ∇DSE ($r^2 = 0.27$; not shown), implying the predominance of the change in latent energy.

3.2 The mechanisms behind the effect of an uncertain change in North Atlantic and Mediterranean SST change

3.2.1 The effects of different warmings of the North Atlantic and Mediterranean Sea

Figure 4 illustrates the effects of the A+M+ and A−M− SST anomaly patterns applied to the three models. The warming of North Atlantic and Mediterranean SSTs is linked to temperature increases over Europe, Asia, and northern Africa (Fig. 4a–c). This rise in temperature across the Northern Hemisphere is associated with a decrease in sea level pressure over the North Atlantic Ocean and the Sahara as well as a strengthening of the westerlies in West Africa and in the central Sahel (Fig. 4d–f). The change in atmospheric circulation is associated with increased precipitation over West Africa (Fig. 4d–f). While the three models show similar anomaly patterns, differences emerge in the intensity of the anomalies, with ARPEGE simulating a more substantial increase in precipitation compared to GA7 and LMDZ, as also seen in Fig. 3. The increase in precipitation over the central Sahel is consistent with precipitation averaged in the CMIP6 ensemble (CMIP6-GLOBAL− in Fig. S1).

A−M− is associated with a strong cooling of the extratropical North Atlantic Ocean, but the change in land temperature is moderate (Fig. 4g–i). The change in precipitation is also moderate over West Africa (Fig. 4j–l). In contrast to Fig. 1f, precipitation does not decrease over the Western Sahel. Figure S7 show that the cooling of the North Atlantic (A−) is not associated with a decrease in precipitation over West Africa. In contrast, moderate warming in the Mediterranean Sea (M−) is associated with an increase in precipitation (Fig. S8), which explains the moderate increase in precipitation in A−M− in the three models.

3.2.2 Addressing uncertainty in Sahel precipitation change

We assess the effects of an uncertain change in North Atlantic and Mediterranean SSTs on the West African atmospheric circulation and precipitation by showing the differences between A+M+ and A−M− in temperature and atmospheric circulation changes.

The strong relative warming of the North Atlantic and Mediterranean SST is associated with a warming over northern Africa, Europe and Asia (Fig. 5a–c) and decreased sea level pressure north of the Sahel (Fig. 5d–f), which allows the monsoon circulation to strengthen and precipitation to increase (Fig. 5d–f). Over the tropical Atlantic Ocean, precipitation increases in the eastern basin, but decreases in the west (not shown), possibly partly driven by the change in atmospheric circulation and precipitation over North and West Africa (Dixon et al. 2018).

Figure 3a shows that the change in precipitation is primarily dynamically driven over the Sahel. These aforementioned results suggest that changes in wind circulation and meridional gradients in sea level pressure and temperature strongly contribute to increased precipitation across West Africa. Changes in soil moisture and local recycling through land–atmosphere coupling also allow for increased precipitation (Koster et al. 2004). The strengthening of the westerlies is associated with a significant increase in precipitation over Africa (*e.g.*, Grodsky et al. 2003; Pu and Cook 2010) and a decrease in precipitation over the western tropical Atlantic (Fig. 5d–f). All models simulate similar patterns in changes in precipitation, temperature, seA−level pressure and wind, and the effects of the North Atlantic and Mediterranean warming can be considered robust over West Africa. Moreover, this is consistent with the known effect of the North Atlantic (Mohino et al. 2011, 2024; Martin and Thorncroft 2014; Monerie et al. 2019) and the Mediterranean Sea (Rowell 2003; Gaetani et al. 2010; Fontaine et al. 2010; Park et al. 2016) on Sahel precipitation. However, the intensity of the precipitation change is uncertain, with ARPEGE simulating, in response to these SST changes, a stronger increase in precipitation, as already noted, and a stronger strengthening of the wind speed than in GA7 and LMDZ (Fig. 5d–f).

The latitude-height profile of the zonal wind speed anomaly reveals a strengthening of low-level westerlies between 10 and 20°N, indicating a northward extension of the monsoon circulation (Fig. 6a–c). The African Easterly Jet (AEJ) (centred around 10°N between 600 and 700 hPa) shifts northward in all models, with decreased wind speed on its southern edge and increased speed on its northern edge, aligning with northward-shifting Sahel precipitation (e.g., Grist and Nicholson 2001) (Fig. 6a–c). The tropical easterly jet (TEJ) also strengthens south of 10°N, promoting West African precipitation, though its representation and precipitation links vary across models (Whittleston et al. 2017). Overall, the northward expansion of westerlies and AEJ shifts support increased West African precipitation.

In addition to the zonal wind, we assess changes in vertical motion. Negative values of omega (vertical wind speed expressed in pressure coordinates) between 5 and 15°N and between 700 and 200 hPa indicate the location of the deep convection over West Africa. Deep mean ascent is maximum South of 10°N (Fig. 6d–f), where precipitation is maximum. Between 10 and 20°N, negative omega values are found below 700 hPa, indicating the location of the shallow circulation. The response to the SST anomalies is a decrease in omega in altitude (800–500 hPa) between 10 and 15°N, indicating enhanced deep convection (Fig. 6d–f),

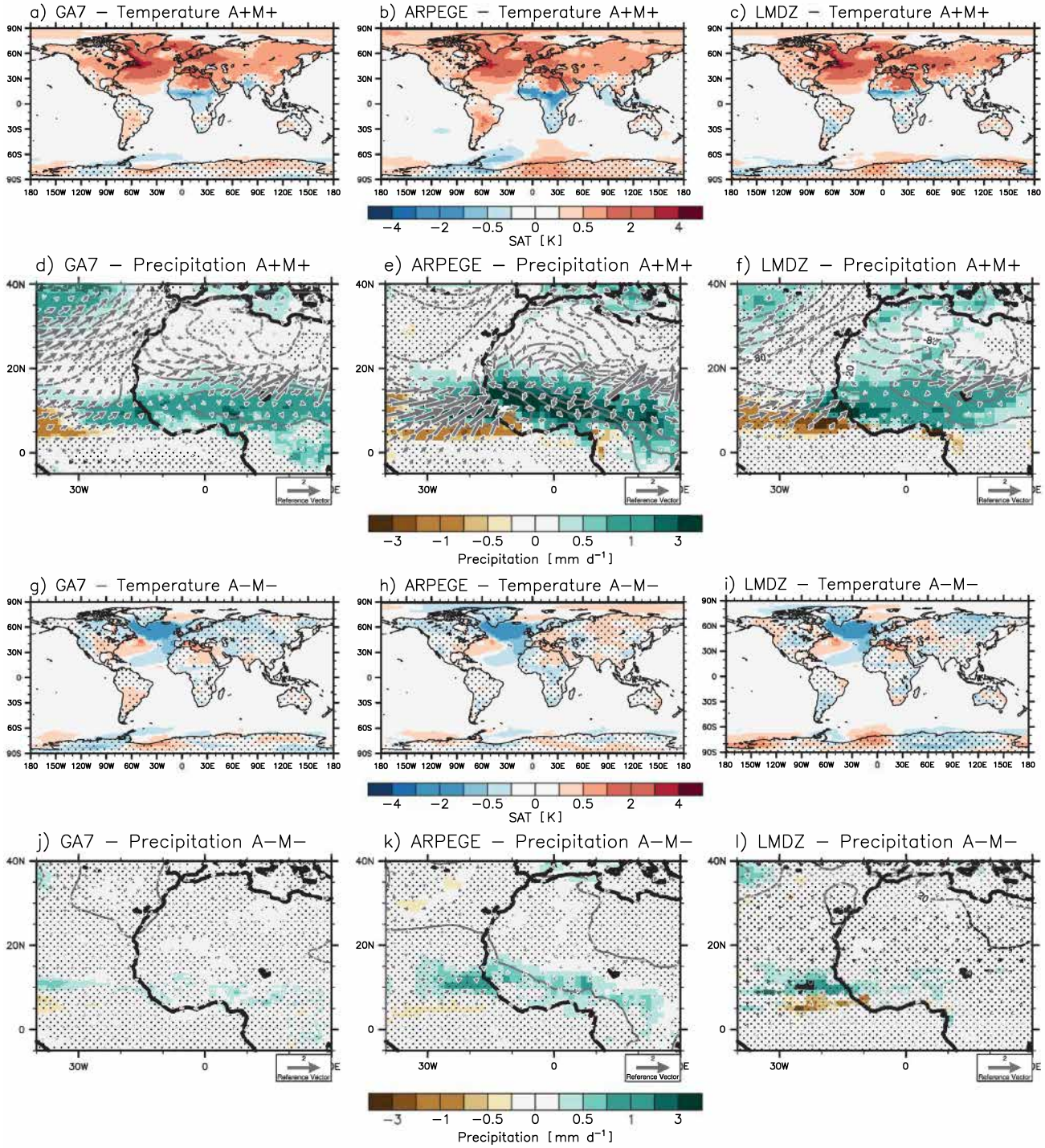

Fig. 4 Effects of the strong increase in North Atlantic and Mediterranean SSTs ([A+M+]–[CTRL]) on **a–c** surface air temperature [K] and **d–f** precipitation [mm d^{-1}] in JAS. Contours indicate the anomalies in sea level pressure [Pa] and vector the change in surface wind speed [m s^{-1}]. Stippling indicates grid points where precipitation anomalies are insignificant according to a Student's t-test at the 95% confidence level. **g–i** as in **a–c** but for the cooling of the North Atlantic and moderate warming of the Mediterranean SST ([A−M−]–[CTRL]). **j–l** as in **d–f** but for the cooling of the North Atlantic and moderate warming of the Mediterranean SST ([A−M−]–[CTRL])

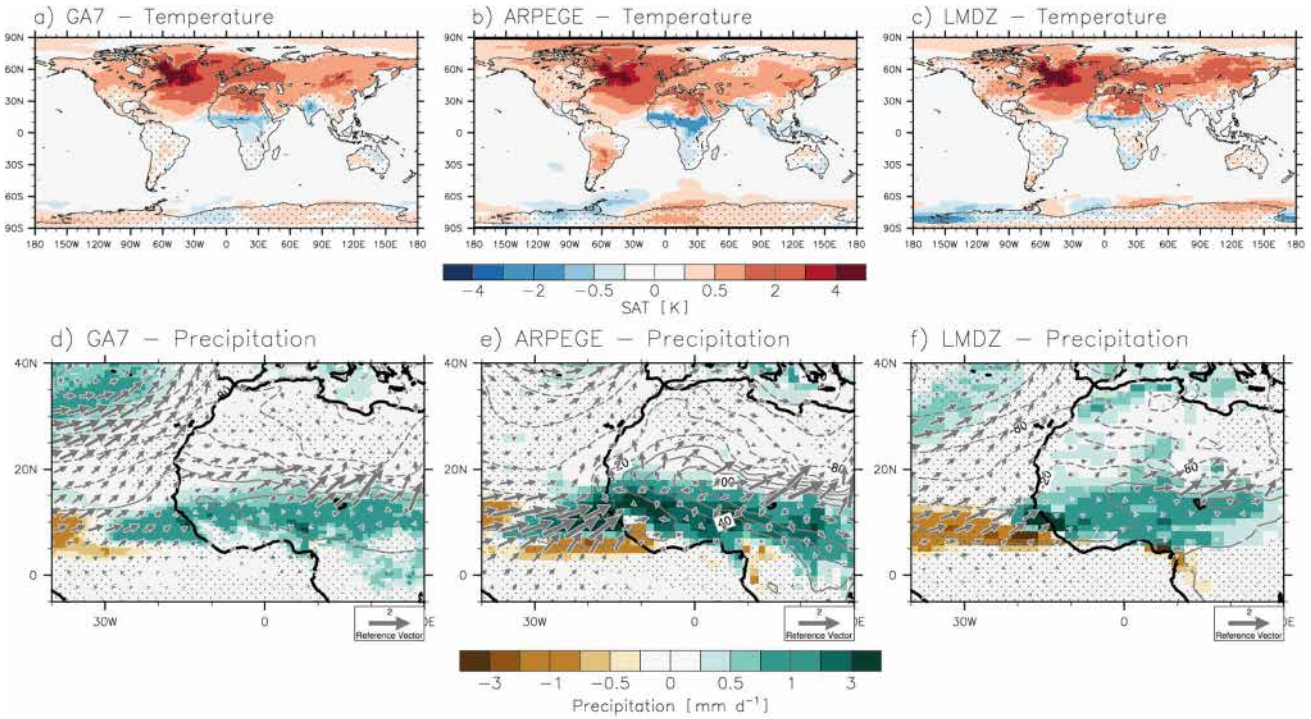

Fig. 5 Effects of the change in North Atlantic and Mediterranean SSTs ([A+M+]–[A−M−]) on **a**–**c** surface air temperature [K] and **d**–**f** precipitation [mm d^{-1}] in JAS. On (**d**–**f**), contours indicate the anomalies in sea level pressure [Pa] and vector the change in surface wind speed [m s^{-1}]. Stippling indicates grid points where precipitation anomalies are insignificant according to a Student's t-test at the 95% confidence level

consistent with increased precipitation and a strengthened monsoon circulation (Fig. 5d–f). In GA7, omega increases over the southern edge of the shallow circulation (~12°–15°N) and decreases over the northern edge of the shallow circulation (~20°–25°N), indicating a northward shift or a narrower shallow circulation that is strengthened over its northern edge (Fig. 6d). In contrast to GA7, LMDZ and ARPEGE show a decrease in omega south of the Sahel (south of 10°N), forming a tripole pattern in the omega anomaly without indicating a clear northward shift in circulation (Fig. 6e–f). ARPEGE exhibits a particularly strong decrease in omega (10°–15°N; 500–200 hPa), suggesting a significant enhancement in deep convection over the Sahel. This aligns with the notably higher increase in precipitation in ARPEGE compared to GA7 and LMDZ.

The change in West African precipitation is associated with changes in the shallow circulation (1000–700 hPa and from 10°N to 20°N) through changes in the Saharan Heat Low (SHL; Lavaysse et al. 2009; Shekhar and Boos 2017; Dixon et al. 2018; Roehrig et al. 2011). We assess circulation associated with the SHL showing wind speed divergence $\nabla_h \cdot u$ at each vertical level, following Shekhar and Boos (2017) (Fig. 6, bottom panels). The climatology shows that wind converges in the lower level (1000–850 hPa) over the Sahel, associated with the monsoon front and Intertropical front, and diverges at higher altitudes (850–500 hPa), in association with the shallow circulation and associated upward motion. In GA7 and LMDZ the low-level $\nabla_h \cdot u$ increases over the southern edge of the shallow circulation and decreases over the northern edge of the shallow circulation, indicating a northward shift in $\nabla_h \cdot u$ in the lower troposphere. A quadrupole in the anomalous $\nabla_h \cdot u$ can then be seen along with a decrease in $\nabla_h \cdot u$ from 10°N to 20°N and an increase in $\nabla_h \cdot u$ north of 20°N, at 850–600 hPa (Fig. 6g–i). This quadrupole is consistent with the effect of a northward shift of the SHL on the West African circulation, as shown by Shekhar and Boos (2017) (their Fig. 8e) and Mutton et al. (2022). However, the anomaly pattern and intensity in $\nabla_h \cdot u$ are model-dependent, with the quadrupole appearing more clearly in GA7 than in LMDZ, with a moderate change in $\nabla_h \cdot u$ over the northern edge of the shallow circulation and 850–700 hPa in LMDZ. ARPEGE exhibits a different behaviour than GA7 and LMDZ, with stronger anomalies in horizontal wind divergence South of 10°N than North of 20°N (Fig. 6h), which could indicate a strengthening of the monsoon circulation rather than a northward shift of the monsoon. Further studies could be devoted to understanding this mechanism using more climate models.

We assessed the effects of North Atlantic and Mediterranean SSTs separately using LMDZ and GA7. Both the increase in North Atlantic and Mediterranean SSTs are

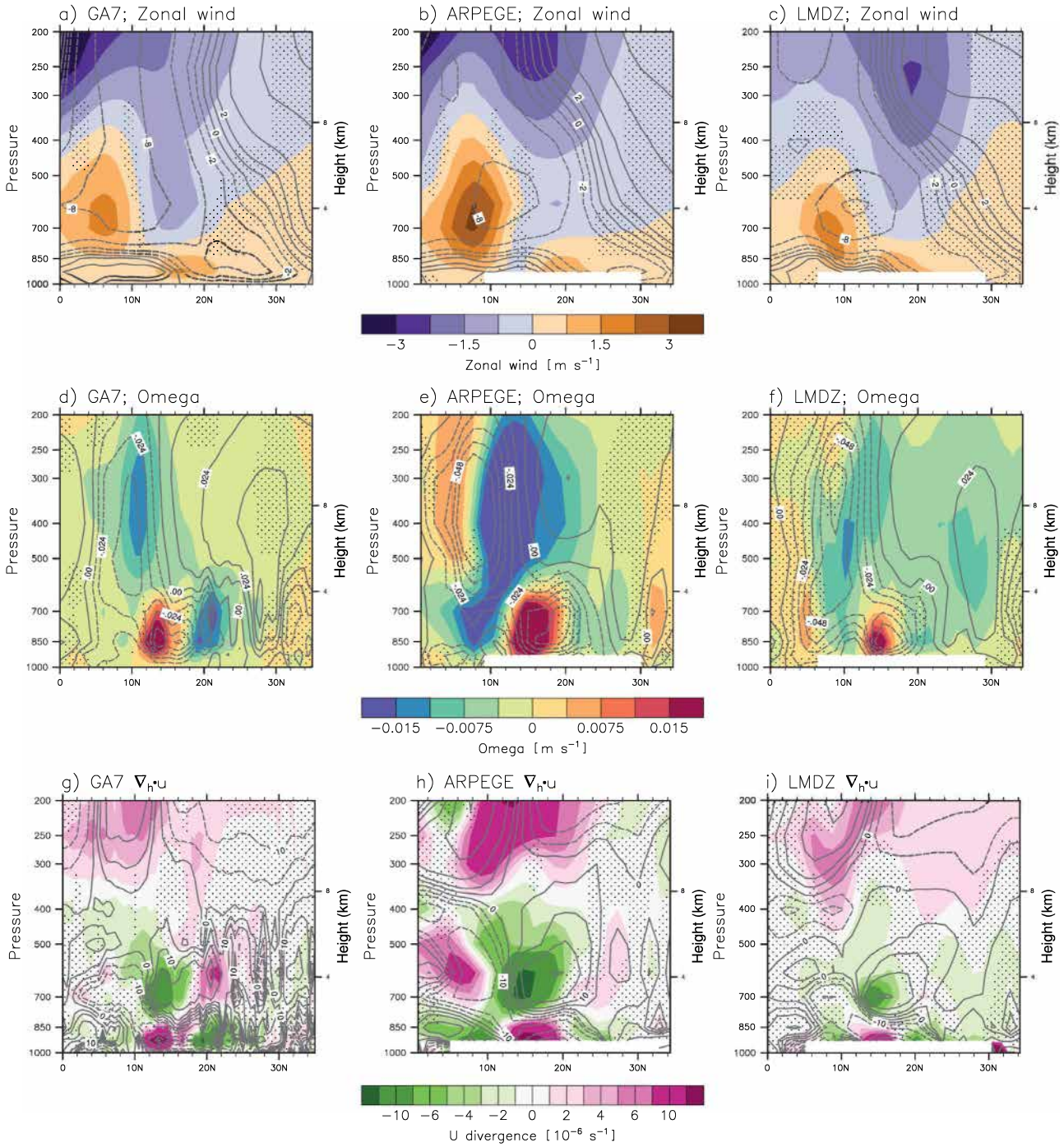

Fig. 6 Latitude-altitude cross sections (averaged between 10°W and 10°E) for the effects of the change in North Atlantic and Mediterranean SSTs ([A+M+]–[A−M−]) on zonal wind [m s^{-1}], omega [Pa s^{-1}], and horizontal wind speed divergence [10^{-6} s^{-1}], in JAS. Contours indicate the climatology (taken from the CTRL experiment). Discontinuous (continuous) lines indicate negative (positive) anomalies. Stippling indicates where anomalies are insignificant according to a Student's t-test at the 95% confidence level

associated with a decrease in sea level pressure over northern Africa and a strengthening of the low-level wind (Figs. S7 and S8). In addition, both the warming of the North Atlantic and Mediterranean SSTs lead to a northward shift of the AEJ and of the monsoon circulation, as well as a quadrupole in horizontal wind speed divergence (Figs. S9 and S10).

We show that the uncertainty in the change in North Atlantic and Mediterranean SST strongly affects precipitation and atmospheric circulation in the Sahel. Our models (GA7, ARPEGE and LMDZ) agree on the change in overall

precipitation and atmospheric circulation. However, there are differences in the magnitude of the precipitation anomalies and the corresponding changes in circulation.

3.3 Impacts of the SST anomaly patterns on storms and heavy precipitation

Heavy and extreme precipitation events strongly contribute to the precipitation climatology, but the long-term changes in such contribution to precipitation totals need to be assessed. We show that in the three models, precipitation events of 10 mm d^{-1} or more, contribute from 30 to 60% to the precipitation climatology in JAS (Fig. S11). The warming of the North Atlantic and Mediterranean SSTs is associated with an increase of ~ 30–40% of the contribution of the heavy precipitation events to the seasonal mean precipitation (Fig. S12). Therefore, we conclude that changes in heavy events contribute to the change in Sahel precipitation. The increase is higher for ARPEGE than for LMDZ and GA7 (Fig. S11). We assessed changes in extreme rainfall (> 20 mm d^{-1}) and reached the same conclusion as for the heavy precipitation events (not shown).

We quantify the change in intense precipitation events by assessing the number of days with heavy precipitation (> 10 mm d^{-1}). Warming in the North Atlantic and Mediterranean Sea is linked to a substantial increase in heavy precipitation events over West Africa in all models (Fig. 7a–c). This implies that an uncertain warming of the North Atlantic and Mediterranean Sea is associated with an uncertain change in the number of very heavy precipitation events across North Africa. The results have substantial implications for African societies and decision-makers. This result is consistent with Mohino et al. (2024), who show a robust effect of the North Atlantic SST on extreme precipitation

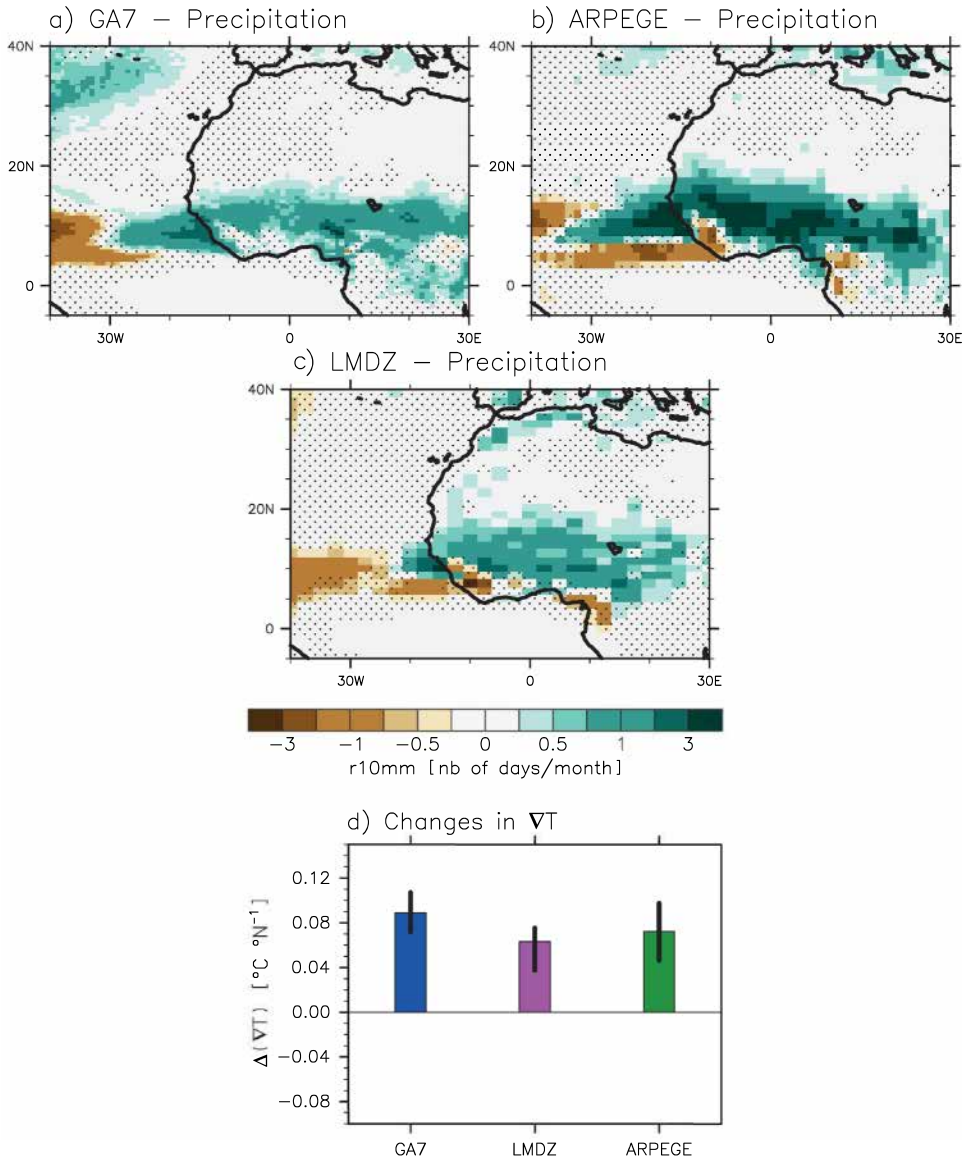

Fig. 7 Effects of an uncertain change in North Atlantic and Mediterranean SST ([A+M+]–[A−M−]) on the number of heavy precipitation events (precipitation > = 10 mm d^{-1}) [number of days per month] for **a** GA7, **b** ARPEGE, and **c** LMDZ. Stippling indicates grid points where anomalies are insignificant according to a Student's t-test at the 95% confidence level. Changes in ∇T [°C °N^{-1}] for GA7 (blue), ARPEGE (green), and LMDZ (magenta). The vertical line denotes the uncertainty, that is, the range between the minimum and maximum values in the change in meridional temperature gradient. A coloured (white) bar shows that anomalies are (are not) statistically significant according to a Student's t-test at the 95% confidence level

events over the Sahel. Similar to the heavy precipitation events, we show an increase in the very heavy precipitation events (20 mm d^{-1}) for each model (Fig. S12). These results show that the impacts of different future trajectories in Sahel precipitation are societally-relevant and would motivate a further study focusing on extreme events.

Changes in extreme rainfall are not only a consequence of mean warming and a thermodynamic increase in humidity. Across the Sahel, intense precipitation events are caused by mesoscale convective systems associated with storms (Lafore et al. 2011; Taylor et al. 2017). Thus, a strengthening of the storm activity can lead to increased extreme precipitation events. As it is considered a proxy for the Sahelian storm activity in CMIP-class models, we link changes in ∇T to changes in heavy precipitation events. We use all simulations and show that, in agreement with Rowell et al. (2021), a strengthening of ∇T is associated with increased precipitation over the Sahel (Fig. S13; $r^2 = 0.53$ between the change in precipitation and ∇T), although the sensitivity of precipitation to ∇T varies among models. Here, we show a robust increase in ∇T due to the increase in the North Atlantic and Mediterranean SSTs across all models (Fig. 7d). (Lafore et al. 2011; Taylor et al. 2017).

4 Limitations and the role of the tropics

According to previous studies (Liu et al. 2014; Monerie et al. 2019; Mohino et al. 2024), we expected an increase in North Atlantic SST to lead to increased Sahel precipitation, and a decrease in North Atlantic SST to result in decreased Sahel precipitation. Here, we show that while the warming of the North Atlantic SST is associated with increased Sahel precipitation, the cooling of the North Atlantic is not associated with a substantial decrease in Sahel precipitation (Fig. 4 bottom line and Fig. 8a).

Further analysis shows that the change in Sahel precipitation driven by a warm North Atlantic is associated with a change in global atmospheric heat transport over the Northern Hemisphere (peaking at 20–30°N, but extending to the equator; Fig. S14) (Schneider et al. 2014). Instead, the cooling of the North Atlantic Ocean (A−) does not lead to a substantial change in heat transport (either over the Northern Hemisphere or at the equator, Fig. S15). Thus, in our AGCM experiments, the cooling of the North Atlantic is not associated with a global redistribution of energy and does not strongly impact the West African monsoon in GA7 and LMDZ. Although A− is not exactly the negative of A+, the discrepancy in the downstream response points to possible non-linearities, which remain unexplained and might complicate the interpretation of our results.

In coupled simulations, a change in North Atlantic temperature is likely to modify SST remotely, with the warming of the North Atlantic SST associated with a cooling of the tropical eastern Pacific Ocean through a strengthening of the Walker circulation (Rodríguez-Fonseca et al. 2009; Ham et al. 2013; Monerie et al. 2020a; Ruprich-Robert et al. 2021; Richter et al. 2023) and cooling of the tropical South Atlantic Ocean via heat redistribution and a northward shift of the Intertropical convergence zone (e.g. Ruprich-Robert et al. 2021). In return, the change in the South tropical Atlantic Ocean, particularly over the cold tongue region, strongly affects West African and Sahel precipitation (Janicot et al. 1998; Losada et al. 2010; Nnamchi and Li 2011; Worou et al. 2020, 2022; Nnamchi et al. 2023). In the atmosphere-only simulations as designed here, SST remains constant over the tropical Atlantic and the eastern Pacific Ocean, leading to a potential underestimation of the effect of the change in Atlantic SST on Sahel precipitation. We test this hypothesis with the atmosphere-only framework and GA7, using an extended pattern of the A− anomaly following Fig. 2b, i.*e.*, including the South tropical Atlantic Ocean, for which SST increases. The inclusion of the warming of the cold tongue region (Fig. 8d) leads to a decrease in precipitation over the Sahel (Fig. 8e), exposing the importance of the tropical Atlantic SST for simulating the full response of precipitation changes to A− and A−M− (Fig. 1f). The role of the tropical Atlantic and tropical mean temperature is consistent with the literature. For example, Giannini et al. (2013) suggest that the increase in tropical mean temperature may affect the amount of energy required to develop deep convection over the tropics and that the warming of the tropical mean SST thus prevents deep convection and precipitation. It remains unclear whether inter-model differences in tropical Atlantic warming are primarily driven by variations in how models simulate changes in extratropical North Atlantic SSTs and their influence on tropical Atlantic SSTs, or by local ocean–atmosphere feedbacks, such as those associated with the development of the cold tongue. Further experiments are also needed to better decipher the role of tropical Atlantic and Pacific SST anomalies in setting this atmospheric transport, following Guilbert et al 2024.

In addition to the absence of remote effects of SST changes on the SST of other oceanic basins, we note that the atmosphere-only simulations could yield an underestimation of changes in Sahel precipitation, because the wind-evaporation-SST feedback (Xie and Philander 1994) is disabled when SSTs are kept constant. In general, when mid-latitude forcing is artificially prevented from affecting tropical SST, we expect a muted Sahelian response (Dixon et al. 2018). Though SST-restoring in coupled models could help include some critical air-sea interactions while preserving SST anomalous patterns, these approaches can also

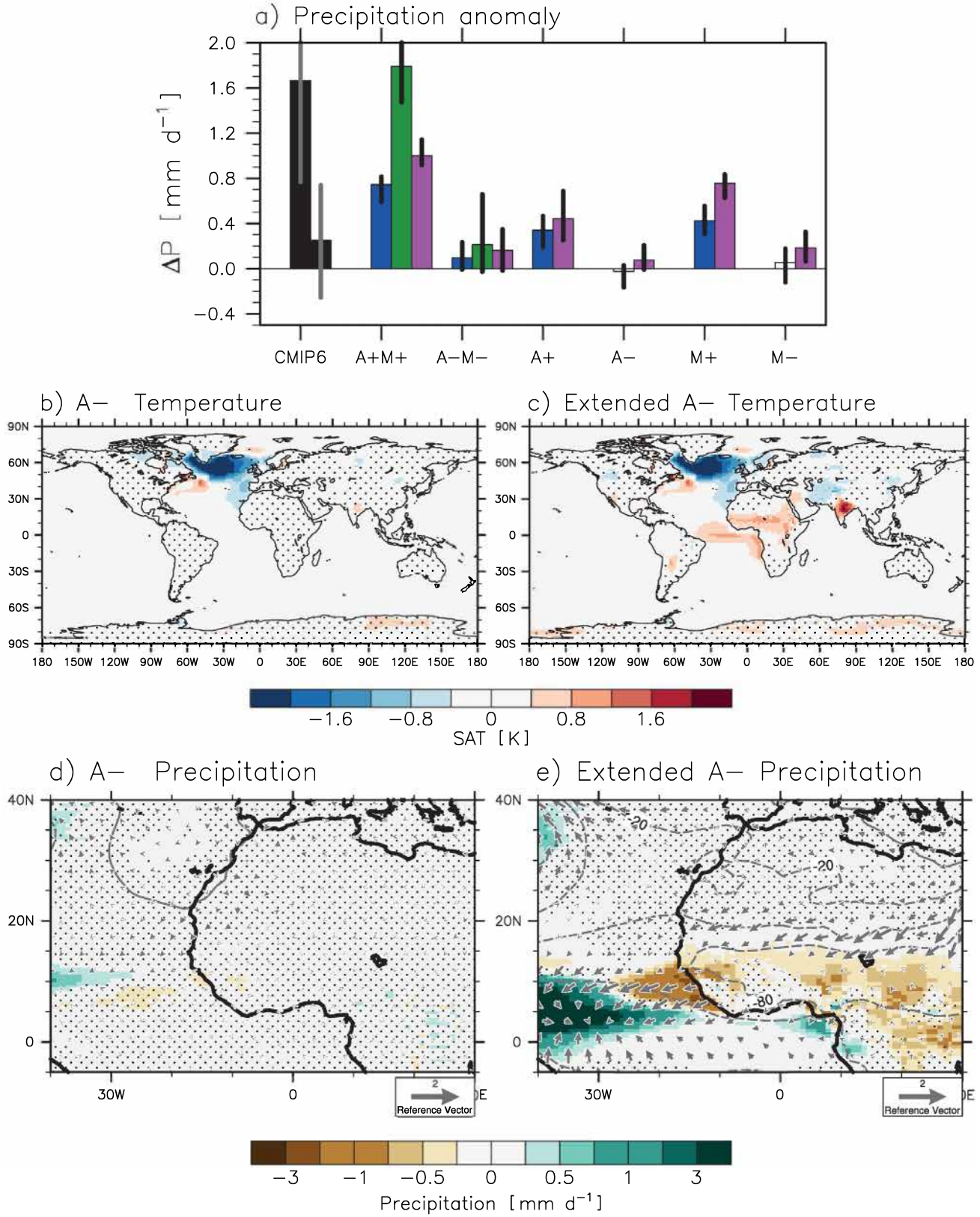
a) Precipitation anomaly
ΔP [mm d−1]
2.0
1.6
1.2
0.8
0.4
0.0
−0.4
CMIP6
A+M+
A−M−
A+
A−
M+
M−
b) A− Temperature
c) Extended A− Temperature
90N
60N
30N
0
30S
60S
90S
180 150W 120W 90W 60W 30W 0 30E 60E 90E 120E 150E 180
−1.6 −0.8 0 0.8 1.6
SAT [K]
d) A− Precipitation
e) Extended A− Precipitation
40N
20N
0
30W
0
Reference Vector
−3 −1 −0.5 0 0.5 1 3
Precipitation [mm d−1]

Fig. 8 **a** Changes in Sahel precipitation [10°W-20°E; 10°N-20°N; mm d^{-1}] in JAS within the CMIP6 ensemble (CMIP6) for the A+M+ and A−M− groups of models. Effects of a warming of the North Atlantic Ocean and Mediterranean SST (A+M+, i.e., [A+M+]–[CTRL]), of cooling of the North Atlantic Ocean and Mediterranean SST (A−M−, i.e., [A−M−]–[CTRL]), of a warming of the North Atlantic SST only (A+, i.e. [A+]–[CTRL]), of cooling of the North Atlantic SST only (A−, i.e. [A−]–[CTRL]), of a warming of the Mediterranean SST only (M+, i.e., [M+]–[CTRL]), and of cooling of the Mediterranean SST only (M−, i.e., [M−]–[CTRL]). The results of GA7 are shown with a blue bar, ARPEGE with a green bar and LMDZ with a magenta bar. The vertical black (grey) lines denote the uncertainty, the range between the minimum and maximum values for each set of experiments (from each model of the two groups of CMIP6 models). A coloured (white) bar shows that anomalies are (are not) statistically significant according to a Student's t-test at the 95% confidence level. Effect of the North Atlantic cooling (A−, i.e., [A−]–[CTRL]) on **b** surface air temperature [K] and **d** precipitation [mm d^{-1}], sea level pressure [Pa] and surface wind speed [m s^{-1}], in JAS, and GA7. **c** and **e**, as in **b** and **d**, but for the effect of the extended A− pattern. On **b**–**e**, stippling indicates grid points where anomalies are insignificant according to a Student's t-test at the 95% confidence level

lead to exaggerating the climate impacts of such patterns (O'Reilly et al. 2023).

In summary, this work tests the effects of two specific, plausible future trajectories for SSTs, and while these can explain a significant proportion of the uncertainty in future changes in Sahel precipitation, more subtle changes in SST (both in pattern and magnitude) exist within CMIP6 and could make a quantitative difference. (Mohino and Losada 2015; Svendsen et al. 2023; Monerie et al. 2018; Neupane and Cook 2013).

5 Conclusion

Future changes in precipitation have major societal implications for the Sahel. However, they are uncertain, and the reasons for this uncertainty are intensely debated. Previous studies have highlighted the role of changes in sea surface temperature (SST) and radiative forcing in future changes in Sahel precipitation (*e.g.*, Mutton et al. 2024). Park et al. (2015, 2016) and Monerie et al. (2023) demonstrate a significant influence on the change in Northern Hemisphere temperatures, particularly in the North Atlantic and Mediterranean regions, while Guilbert et al. (2024) highlight the role of the interhemispheric temperature contrast and the equatorial Pacific Sea Surface Temperature (SST). In addition to SST, uncertainty in the future change of temperature gradients at the regional scale also affects the uncertainty in projections of heavy precipitation events (Rowell et al. 2021). Following Monerie et al. (2023), we assess the specific role of an uncertain change in the North Atlantic and Mediterranean SST on Sahel precipitation using a mechanistic approach, targeted sensitivity experiments and three atmosphere models. We assume that the uncertainty in Sahel precipitation change is closely linked to the different SST changes among the CMIP6 models. We therefore apply these SST anomalies to better understand uncertainty in Sahel precipitation change.

We show that understanding the future changes in North Atlantic and Mediterranean SSTs, as well as their effects on Sahel precipitation, is crucial for better understanding the future changes in Sahel precipitation during the monsoon season. We demonstrate that warming of the North Atlantic and the Mediterranean Sea is linked to increased precipitation over the Sahel, primarily through a strengthening and northward shift of the atmospheric circulation over West Africa. We demonstrate that the effects of SST anomaly patterns on changes in large-scale energy gradients enable the monsoon circulation to strengthen and precipitation to increase. Therefore, we confirm that an uncertain change in North Atlantic and Mediterranean SSTs contributes to uncertainty in future changes of Sahel precipitation.

Yet, the uncertainty in SST projections is not the only source of disagreement in Sahel rainfall projections, as demonstrated here by using three atmospheric models (ARPEGE, GA7, and LMDZ). We show substantial differences between models in simulating the effects of the same SST anomaly pattern on Sahel precipitation. For example, ARPEGE produces Sahel precipitation anomalies approximately twice as large as those in GA7 and LMDZ. ARPEGE simulates stronger changes in Sahel precipitation than the other models, along with particularly strong changes in the meridional gradient in moist static energy, atmospheric circulation and vertical velocity. Unlike GA7 and LMDZ, ARPEGE simulates a strengthening of the monsoon circulation, rather than a clear northward shift. We conclude that there is significant inter-model diversity in the response of the Sahel precipitation to SST anomalies. Further work devoted to better understanding this diversity of response to SST anomalies might benefit from a larger number of atmospheric models, using additional process-based metrics such as for soil-moisture feedback, and addressing the role of models' horizontal resolution and parameterisations (*e.g.*, Hill et al. 2017; Dixon et al. 2019). Furthermore, we demonstrate variations in precipitation bias patterns and magnitudes among the three models. We also propose that these discrepancies could be attributed to the way precipitation is represented in each model. Both the diversity across models and the non-linearity of the response may also suggest a substantial sensitivity of the regional response to the climatological background state.

From our results, we conclude that reducing uncertainty in Sahel precipitation change implies a better understanding of the future changes in SST over the Northern Hemisphere and how these changes in North Atlantic and Mediterranean SST affect Sahel precipitation in climate models.

Besides the summer mean, we show that uncertainty in the future change in the North Atlantic and Mediterranean SSTs leads to an uncertain estimate in the future change of the intense weather events (measured as the number of days with more than 10 and 20 mm d^{-1}), due to an uncertain change in regional temperature gradients (following Rowell et al. 2021). These intense weather events are societally relevant, as they have a substantial impact on communities, agriculture, and the economy, contributing to crop damage and flooding.

A limitation of the study is the use of atmosphere-only simulations. Atmosphere-only simulations are powerful tools for assessing the effects of specific SST anomaly patterns, but they do not provide a means to evaluate the connections between oceanic basins. We argue that the remote effects of extratropical SSTs on tropical SSTs are crucial for capturing the full effect of changes in North Atlantic SSTs and that one may be underestimating their role. We suggest that future studies address this issue using multiple coupled ocean–atmosphere climate model simulations.

Uncertainty in precipitation change in the Sahel has not decreased over time, with similar uncertainties in CMIP3 (Randall et al. 2007), CMIP5 (Taylor et al. 2012) and CMIP6 (Eyring et al. 2016), as reported in (Rodríguez-Fonseca et al. 2015) and Monerie et al (2020a, b), among others. We suggest that the time has come to develop a new Model Intercomparison Project (MIP) targeting SST anomaly patterns to better understand future changes in tropical precipitation. Additionally, one could utilise the outcomes of the Green Function MIP (Bloch-Johnson et al. 2024).

Further work could be devoted to understanding the impact of an uncertain change in extratropical SST on precipitation and temperature extremes. For example, Badji et al. (2022) show a decadal variability of precipitation extremes over the western Sahel in relation to the decadal variability of North Atlantic SST (Atlantic Multidecadal Variability). Another way forward in understanding the future change in Sahel precipitation is to develop a constraint framework, based on the future change in SST, to reduce the uncertainty in Sahel precipitation change towards the end of the twenty-first century, based on emergent constraint (Chen et al. 2022) or reducing uncertainty in changes in relevant SSTs (Qasmi and Ribes 2025).

Supplementary Information The online version contains supplementary material available at https://doi.org/10.1007/s00382-025-07835-0.

Acknowledgements We acknowledge the World Climate Research Programme, which, through its Working Group on Coupled Modelling, coordinated and promoted CMIP6. We thank the climate modeling groups for producing and making available their model output, the Earth System Grid Federation (ESGF) for archiving the data and providing access, and the multiple funding agencies who support CMIP6 and ESGF. EM received funding from the Spanish Ministry of Science and Innovation DISTROPIA and OFF projects (grants no. PID2021-125806NB-I00 and TED2021-130106B-I00) and the "Recualificación del Sistema Universitario Español para 2021–2023" call from the Universidad Complutense de Madrid, which has been financed by the Ministry of Universities with funds from the Next Generation of the European Union. PAM received funding from the European Union's Horizon 2020 research and innovation programme under grant agreement No 823988 (ESIWACE2). MB received funding from NSF award AGS-2402470. We thank Lister Grenville for his continuous support in running the GA7 simulations. This work used the ARCHER2 UK National Supercomputing Service (https://www.archer2.ac.uk). The LMDZ simulations were provided with computing HPC and storage resources by GENCI at TGCC, thanks to the grant 2025-A0170107403 on the supercomputer Joliot Curie's ROME partition. JM and EM would like to thank Fréderic Hourdin and Ionela Musat (LMD-IPSL) for technical support in setting up the LMDZ simulations. We thank the three anonymous reviewers and Ross Dixon for their comments and suggestions.

Author contributions PAM wrote the first draft of the manuscript and EM, JM, MB, BP, MPM contributed to the writing and commented on previous versions of the manuscript. All authors read and approved the final manuscript. EM performed the simulations with LMDZ, MPM performed the simulations with ARPEGE, and PAM performed the simulations with GA7. PAM performed the analyses.

Data availability CMIP6 GCM output is available from public repositories, including https://esgf-index1.ceda.ac.uk/search/cmip6-ceda/. GA7, LMDZ, and ARPEGE model datasets are from the corresponding author on reasonable request.

Declarations

Conflict of interest The authors declare that they have no conflict of interest.

References

Audu EO, Dixon RD, Diallo I (2024) Understanding the zonal variability in projections of Sahel precipitation. Geophys Res Lett 51:e2024GL110177

Badji A, Mohino E, Diakhaté M et al (2022) Decadal variability of rainfall in Senegal: beyond the total seasonal amount. J Clim 35:5339–5358. https://doi.org/10.1175/JCLI-D-21-0699.1

Best MJ, Pryor M, Clark DB et al (2011) The joint UK land environment simulator (JULES), model description – Part 1: energy and water fluxes. Geosci Model Dev 4:677–699. https://doi.org/10.5194/gmd-4-677-2011

Biasutti M (2013) Forced Sahel rainfall trends in the CMIP5 archive. J Geophys Res Atmos 118:1613–1623. https://doi.org/10.1002/jgrd.50206

Bloch-Johnson J, Rugenstein MAA, Alessi MJ et al (2024) The green's function model intercomparison project (GFMIP) protocol. J Adv Model Earth Syst 16:e2023MS003700

Boucher O, Servonnat J, Albright AL et al (2020) Presentation and evaluation of the IPSL-CM6A−LR climate model. J Adv Model Earth Syst 12:e2019MS002010

Caesar L, Rahmstorf S, Robinson A et al (2018) Observed fingerprint of a weakening Atlantic Ocean overturning circulation. Nature 556:191–196. https://doi.org/10.1038/s41586-018-0006-5

Cao J, Wang B, Yang Y-M et al (2018) The NUIST Earth System Model~(NESM) version 3: description and preliminary evaluation. Geosci Model Dev 11:2975–2993. https://doi.org/10.5194/gmd-11-2975-2018

Chadwick R, Good P, Willett K (2016) A simple moisture advection model of specific humidity change over land in response to SST warming. J Clim 29:7613–7632. https://doi.org/10.1175/JCLI-D-16-0241.1

Chen Z, Zhou T, Chen X et al (2022) Observationally constrained projection of Afro-Asian monsoon precipitation. Nat Commun 13:2552. https://doi.org/10.1038/s41467-022-30106-z

Cherchi A, Fogli PG, Lovato T et al (2019) Global mean climate and main patterns of variability in the CMCC-CM2 coupled model. J Adv Model Earth Syst 11:185–209

Danabasoglu G, Lamarque J-F, Bacmeister J et al (2020) The community earth system model version 2 (CESM2). J Adv Model Earth Syst 12:e2019MS001916. https://doi.org/10.1029/2019MS001916

Dixon RD, Vimont DJ, Daloz AS (2018) The relationship between tropical precipitation biases and the Saharan heat low bias in CMIP5 models. Clim Dyn 50:3729–3744. https://doi.org/10.1007/s00382-017-3838-z

Dixon RD, Peyrillé P, Guichard F (2019) Sahelian precipitation change induced by SST increase: the contrasting roles of regional and larger-scale drivers. Geophys Res Lett 46:11378–11387

Dong B, Sutton R (2015) Dominant role of greenhouse-gas forcing in the recovery of Sahel rainfall. Nat Clim Chang 5:757–760. https://doi.org/10.1038/nclimate2664

Dong X, Jin J, Liu H et al (2021) CAS-ESM2.0 model datasets for the CMIP6 ocean model intercomparison project phase 1 (OMIP1). Adv Atmos Sci 38:307–316. https://doi.org/10.1007/s00376-020-0150-3

Dunne JP, Horowitz LW, Adcroft AJ et al (2020) The GFDL earth system model version 4.1 (GFDL-ESM 4.1): overall coupled model description and simulation characteristics. J Adv Model Earth Syst 12:e2019MS002015

Ekolu J, Dieppois B, Tramblay Y et al (2024) Variability in flood frequency in sub-Saharan Africa: the role of large-scale climate modes of variability and their future impacts. J Hydrol 640:131679

Eltahir EAB, Gong C (1996) Dynamics of wet and dry years in West Africa. J Clim 9:1030–1042

Eyring V, Bony S, Meehl GA et al (2016) Overview of the coupled model intercomparison project phase 6 (CMIP6) experimental design and organization. Geosci Model Dev 9:1937–1958. https://doi.org/10.5194/gmd-9-1937-2016

Fontaine B, Philippon N (2000) Seasonal evolution of boundary layer heat content in the West African monsoon from the NCEP/NCAR reanalysis (1968–1998). Int J Climatol 20:1777–1790

Fontaine B, GarciA−Serrano J, Roucou P et al (2010) Impacts of warm and cold situations in the Mediterranean basins on the West African monsoon: observed connection patterns (1979–2006) and climate simulations. Clim Dyn 35:95–114. https://doi.org/10.1007/s00382-009-0599-3

Gaetani M, Fontaine B, Roucou P, Baldi M (2010) Influence of the Mediterranean Sea on the West African monsoon: intraseasonal variability in numerical simulations. J Geophys Res Atmos. https://doi.org/10.1029/2010JD014436

Gaetani M, Flamant C, Bastin S et al (2017) West African monsoon dynamics and precipitation: the competition between global SST warming and CO2 increase in CMIP5 idealized simulations. Clim Dyn 48:1353–1373. https://doi.org/10.1007/s00382-016-3146-z

Giannini A, Salack S, Lodoun T et al (2013) A unifying view of climate change in the Sahel linking intrA−seasonal, interannual and longer time scales. Environ Res Lett 8:24010. https://doi.org/10.1088/1748-9326/8/2/024010

Golaz J-C, Caldwell PM, Van Roekel LP et al (2019) The DOE E3SM coupled model version 1: overview and evaluation at standard resolution. J Adv Model Earth Syst 11:2089–2129. https://doi.org/10.1029/2018MS001603

Grist JP, Nicholson SE (2001) A study of the dynamic factors influencing the rainfall variability in the West African Sahel. J Clim 14:1337–1359. https://doi.org/10.1175/1520-0442(2001)014%3c1337:ASOTDF%3e2.0.CO;2

Grodsky SA, Carton JA, Nigam S (2003) Near surface westerly wind jet in the Atlantic ITCZ. Geophys Res Lett. https://doi.org/10.1029/2003GL017867

Guilbert M, Terray P, Mignot J et al (2024) Interhemispheric temperature gradient and Equatorial Pacific SSTs drive Sahel monsoon uncertainties under global warming. J Clim 37:1033–1052

Hajima T, Watanabe M, Yamamoto A et al (2020) Development of the MIROC-ES2L Earth system model and the evaluation of biogeochemical processes and feedbacks. Geosci Model Dev 13:2197–2244. https://doi.org/10.5194/gmd-13-2197-2020

Ham Y-G, Kug J-S, Park J-Y (2013) Two distinct roles of Atlantic SSTs in ENSO variability: North Tropical Atlantic SST and Atlantic Niño. Geophys Res Lett 40:4012–4017. https://doi.org/10.1002/grl.50729

Held IM, Soden BJ (2006) Robust responses of the hydrological cycle to global warming. J Clim 19:5686–5699. https://doi.org/10.1175/JCLI3990.1

Held IM, Guo H, Adcroft A et al (2019) Structure and performance of GFDL's CM4.0 climate model. J Adv Model Earth Syst 11:3691–3727

Herman RJ, Giannini A, Biasutti M, Kushnir Y (2020) The effects of anthropogenic and volcanic aerosols and greenhouse gases on twentieth century Sahel precipitation. Sci Rep 10:12203. https://doi.org/10.1038/s41598-020-68356-w

Hill SA, Ming Y, Held IM, Zhao M (2017) A moist static energy budget-based analysis of the Sahel rainfall response to uniform oceanic warming. J Clim 30:5637–5660. https://doi.org/10.1175/JCLI-D-16-0785.1

Hirasawa H, Kushner PJ, Sigmond M et al (2022) Evolving Sahel rainfall response to anthropogenic aerosols driven by shifting regional oceanic and emission influences. J Clim 35:3181–3193. https://doi.org/10.1175/JCLI-D-21-0795.1

Hourdin F, Rio C, Grandpeix J-Y et al (2020) LMDZ6A: the atmospheric component of the IPSL climate model with improved and better tuned physics. J Adv Model Earth Syst 12:e2019MS001892

janicot s, harzallah a, fontaine b, moron v (1998) West African monsoon dynamics and eastern equatorial Atlantic and pacific SST anomalies (1970–88). j Clim 11:1874–1882

Jeong H, Park H-S, Kang SM, Chung E-S (2025) The greater role of Southern Ocean warming compared to Arctic Ocean warming in shifting future tropical rainfall patterns. Nat Commun 16:2790. https://doi.org/10.1038/s41467-025-57654-4

Kelley M, Schmidt GA, Nazarenko LS et al (2020) GISS-E2.1: configurations and climatology. J Adv Model Earth Syst 12:e2019MS002025. https://doi.org/10.1029/2019MS002025

Knight JR, Allan RJ, Folland CK et al (2005) A signature of persistent natural thermohaline circulation cycles in observed climate. Geophys Res Lett. https://doi.org/10.1029/2005GL024233

Koster RD, Dirmeyer PA, Guo Z et al (2004) Regions of strong coupling between soil moisture and precipitation. Science 305:1138–1140. https://doi.org/10.1126/science.1100217

Krinner G, Viovy N, de Noblet-Ducoudré N et al (2005) A dynamic global vegetation model for studies of the coupled atmosphere-biosphere system. Glob Biogeochem Cycles. https://doi.org/10.1029/2003GB002199

Kuhlbrodt T, Jones CG, Sellar A et al (2018) The low-resolution version of HadGEM3 GC3.1: development and evaluation for global climate. J Adv Model Earth Syst 10:2865–2888. https://doi.org/10.1029/2018MS001370

Lafore J-P, Flamant C, Guichard F et al (2011) Progress in understanding of weather systems in West Africa. Atmos Sci Lett 12:7–12. https://doi.org/10.1002/asl.335

Lavaysse C, Flamant C, Janicot S et al (2009) Seasonal evolution of the West African heat low: a climatological perspective. Clim Dyn 33:313–330. https://doi.org/10.1007/s00382-009-0553-4

Lee J, Kim J, Sun M−A et al (2020) Evaluation of the Korea Meteorological Administration advanced community earth-system model (K-ACE). AsiA−Pac J Atmos Sci 56:381–395. https://doi.org/10.1007/s13143-019-00144-7

Li J, Bao Q, Liu Y et al (2019) Evaluation of FAMIL2 in simulating the climatology and seasonal-to-interannual variability of tropical cyclone characteristics. J Adv Model Earth Syst 11:1117–1136

Li L, Yu Y, Tang Y et al (2020) The flexible global ocean-atmosphere-land system model grid-point version 3 (FGOALS-g3): description and evaluation. J Adv Model Earth Syst 12:e2019MS002012. https://doi.org/10.1029/2019MS002012

Liu Y, Chiang JCH, Chou C, Patricola CM (2014) Atmospheric teleconnection mechanisms of extratropical North Atlantic SST influence on Sahel rainfall. Clim Dyn 43:2797–2811. https://doi.org/10.1007/s00382-014-2094-8

Liu W, Fedorov AV, Xie S-P, Hu S (2020) Climate impacts of a weakened Atlantic meridional overturning circulation in a warming climate. Sci Adv 6:eaaz4876. https://doi.org/10.1126/sciadv.aaz4876

Losada T, Rodríguez-Fonseca B, Janicot S et al (2010) A multi-model approach to the Atlantic Equatorial mode: impact on the West African monsoon. Clim Dyn 35:29–43. https://doi.org/10.1007/s00382-009-0625-5

Martin ER, Thorncroft C (2014) Sahel rainfall in multimodel CMIP5 decadal hindcasts. Geophys Res Lett 41:2169–2175. https://doi.org/10.1002/2014GL059338

Marvel K, Biasutti M, Bonfils C (2020) Fingerprints of external forcing agents on Sahel rainfall: aerosols, greenhouse gases, and model-observation discrepancies. Environ Res Lett 15:084023

Masson V, Le Moigne P, Martin E et al (2013) The SURFEXv7.2 land and ocean surface platform for coupled or offline simulation of earth surface variables and fluxes. Geosci Model Dev 6:929–960. https://doi.org/10.5194/gmd-6-929-2013

Mohino E, Losada T (2015) Impacts of the Atlantic Equatorial Mode in a warmer climate. Clim Dyn 45:2255–2271. https://doi.org/10.1007/s00382-015-2471-y

Mohino E, Janicot S, Bader J (2011) Sahel rainfall and decadal to multi-decadal sea surface temperature variability. Clim Dyn 37:419–440. https://doi.org/10.1007/s00382-010-0867-2

Mohino E, Monerie P-A, Mignot J et al (2024) Impact of Atlantic multidecadal variability on rainfall intensity distribution and timing of the West African monsoon. Earth Syst Dyn 15:15–40. https://doi.org/10.5194/esd-15-15-2024

Monerie P-A, Sanchez-Gomez E, Boé J (2016) On the range of future Sahel precipitation projections and the selection of a sub-sample of CMIP5 models for impact studies. Clim Dyn. https://doi.org/10.1007/s00382-016-3236-y

Monerie P-A, Oudar T, Sanchez-Gomez E (2018) Respective impacts of Arctic sea ice decline and increasing greenhouse gases concentration on Sahel precipitation. Clim Dyn. https://doi.org/10.1007/s00382-018-4488-5

Monerie P-A, Robson J, Dong B et al (2019) Effect of the Atlantic Multidecadal Variability on the Global Monsoon. Geophys Res Lett 46:1765–1775

Monerie P-A, Robson J, Dong B, Hodson D (2020a) Role of the Atlantic multidecadal variability in modulating East Asian climate. Clim Dyn. https://doi.org/10.1007/s00382-020-05477-y

Monerie P-A, Wainwright CM, Sidibe M, Akinsanola AA (2020b) Model uncertainties in climate change impacts on Sahel precipitation in ensembles of CMIP5 and CMIP6 simulations. Clim Dyn 55:1385–1401. https://doi.org/10.1007/s00382-020-05332-0

Monerie P-A, Wilcox LJ, Turner AG (2022) Effects of anthropogenic aerosol and greenhouse gas emissions on Northern Hemisphere monsoon precipitation: mechanisms and uncertainty. J Clim. https://doi.org/10.1175/JCLI-D-21-0412.1

Monerie P-A, Biasutti M, Mignot J et al (2023) Storylines of Sahel precipitation change: roles of the North Atlantic and Euro-Mediterranean temperature. J Geophys Res Atmos 128:e2023JD038712

Mutton H, Chadwick R, Collins M et al (2022) The impact of the direct radiative effect of increased CO2 on the West African monsoon. J Clim 35:2441–2458. https://doi.org/10.1175/JCLI-D-21-0340.1

Mutton H, Chadwick R, Collins M et al (2024) The impact of a uniform ocean warming on the West African monsoon. Clim Dyn 62:103–122. https://doi.org/10.1007/s00382-023-06898-1

Neupane N, Cook KH (2013) A nonlinear response of Sahel rainfall to Atlantic warming. J Clim 26:7080–7096

Nicholson SE (2013) The West African Sahel: a review of recent studies on the rainfall regime and its interannual variability. ISRN Meteorol 2013:1–32. https://doi.org/10.1155/2013/453521

Nnamchi HC, Li J (2011) Influence of the South Atlantic Ocean dipole on West African summer precipitation. J Clim 24:1184–1197

Nnamchi HC, Farneti R, Keenlyside NS et al (2023) Pan-Atlantic decadal climate oscillation linked to ocean circulation. Commun Earth Environ 4:121. https://doi.org/10.1038/s43247-023-00781-x

O'Neill BC, Tebaldi C, van Vuuren DP et al (2016) The scenario model intercomparison project (ScenarioMIP) for CMIP6. Geosci Model Dev 9:3461–3482. https://doi.org/10.5194/gmd-9-3461-2016

O'Reilly CH, Patterson M, Robson J et al (2023) Challenges with interpreting the impact of Atlantic Multidecadal Variability using SST-restoring experiments. NPJ Clim Atmos Sci 6:14. https://doi.org/10.1038/s41612-023-00335-0

Osgood D, Blakeley SL, Ouni S et al (2024) Climate variability through the lens of applied weather index insurance in Senegal-a novel perspective on the implications of decadal variation. Front Clim. https://doi.org/10.3389/fclim.2024.1281623

Park J-Y, Bader J, Matei D (2015) Northern-hemispheric differential warming is the key to understanding the discrepancies in the projected Sahel rainfall. Nat Commun 6:5985

Park J, Bader J, Matei D (2016) Anthropogenic Mediterranean warming essential driver for present and future Sahel rainfall. Nat Clim Chang 6:941–945

Pu B, Cook KH (2010) Dynamics of the West African westerly jet. J Clim 23:6263–6276

Qasmi S, Ribes A (2025) Reducing uncertainty in local temperature projections. Sci Adv 8:eabo6872. https://doi.org/10.1126/sciadv.abo6872

Randall DA, Wood RA, Bony S, et al (2007) Climate models and their evaluation. In: Climate change 2007: The physical science basis.

Contribution of Working Group I to the Fourth Assessment Report of the IPCC (FAR). Cambridge University Press, pp 589–662
Reynolds RW, Smith TM, Liu C et al (2007) Daily high-resolution-blended analyses for sea surface temperature. J Clim 20:5473–5496
Richter I, Kosaka Y, Kido S, Tokinaga H (2023) The tropical Atlantic as a negative feedback on ENSO. Clim Dyn 61:309–327. https://doi.org/10.1007/s00382-022-06582-w
Rodríguez-Fonseca B, Polo I, GarcíA−Serrano J et al (2009) Are Atlantic Niños enhancing Pacific ENSO events in recent decades? Geophys Res Lett. https://doi.org/10.1029/2009GL040048
Rodríguez-Fonseca B, Mohino E, Mechoso CR et al (2015) Variability and predictability of West African droughts: a review on the role of sea surface temperature anomalies. J Clim 28:4034–4060
Roehrig R, Chauvin F, Lafore J-P (2011) 10–25-day intraseasonal variability of convection over the Sahel: a role of the Saharan Heat Low and midlatitudes. J Clim 24:5863–5878. https://doi.org/10.1175/2011JCLI3960.1
Roehrig R, Beau I, Saint-Martin D et al (2020) The CNRM global atmosphere model ARPEGE-climat 6.3: description and evaluation. J Adv Model Earth Syst 12:e2020MS002075
Rowell DP (2003) The impact of Mediterranean SSTs on the Sahelian rainfall season. J Clim 16:849–862. https://doi.org/10.1175/1520-0442(2003)016%3c0849:TIOMSO%3e2.0.CO;2
Rowell DP, Fitzpatrick RGJ, Jackson LS, Redmond G (2021) Understanding intermodel variability in future projections of a Sahelian storm proxy and Southern Saharan warming. J Clim 34:509–525. https://doi.org/10.1175/JCLI-D-20-0382.1
Ruprich-Robert Y, Moreno-Chamarro E, Levine X et al (2021) Impacts of Atlantic multidecadal variability on the tropical Pacific: a multi-model study. Npj Clim Atmos Sci 4:33. https://doi.org/10.1038/s41612-021-00188-5
Sanogo S, Fink AH, Omotosho JA et al (2015) Spatio-temporal characteristics of the recent rainfall recovery in west Africa. Int J Climatol 35:4589–4605. https://doi.org/10.1002/joc.4309
Schneider T, Bischoff T, Haug GH (2014) Migrations and dynamics of the intertropical convergence zone. Nature 513:45–53. https://doi.org/10.1038/nature13636
Séférian R, Nabat P, Michou M et al (2019) Evaluation of CNRM earth system model, CNRM−ESM2-1: role of earth system processes in present-day and future climate. J Adv Model Earth Syst 11:4182–4227. https://doi.org/10.1029/2019MS001791
Shekhar R, Boos WR (2017) Weakening and shifting of the Saharan shallow meridional circulation during wet years of the West African monsoon. J Clim 30:7399–7422. https://doi.org/10.1175/JCLI-D-16-0696.1
Sillmann J, Kharin VV, Zhang X et al (2013) Climate extremes indices in the CMIP5 multimodel ensemble: part 1. Model evaluation in the present climate. J Geophys Res Atmos 118:1716–1733. https://doi.org/10.1002/jgrd.50203
Stouffer R (2019) U of Arizona MCM−UA−1–0 model output prepared for CMIP6 CMIP
Svendsen L, Rodríguez-Fonseca B, Mohino E et al (2023) Tropical atmospheric response of Atlantic Niños to changes in the ocean background state. Geophys Res Lett 50:e2023GL104332
Swapna P, Krishnan R, Sandeep N et al (2018) Long-term climate simulations using the IITM Earth System Model (IITM−ESMv2) with focus on the South Asian monsoon. J Adv Model Earth Syst 10:1127–1149
Tatebe H, Ogura T, Nitta T et al (2019) Description and basic evaluation of simulated mean state, internal variability, and climate sensitivity in MIROC6. Geosci Model Dev 12:2727–2765. https://doi.org/10.5194/gmd-12-2727-2019
Taylor KE, Stouffer RJ, Meehl GA (2012) An overview of CMIP5 and the experiment design. Bull Am Meteorol Soc 93:485–498
Taylor CM, Belušić D, Guichard F et al (2017) Frequency of extreme Sahelian storms tripled since 1982 in satellite observations. Nature 544:475–478. https://doi.org/10.1038/nature22069
Volodin EM, Mortikov EV, Kostrykin SV et al (2017) Simulation of the present-day climate with the climate model INMCM5. Clim Dyn 49:3715–3734. https://doi.org/10.1007/s00382-017-3539-7
Walters D, Baran AJ, Boutle I et al (2019) The met office unified model global atmosphere 7.0/7.1 and JULES global land 7.0 configurations. Geosci Model Dev 12:1909–1963. https://doi.org/10.5194/gmd-12-1909-2019
Wang Y-C, Hsu H-H, Chen C-A et al (2021) Performance of the Taiwan Earth system model in simulating climate variability compared with observations and CMIP6 model simulations. J Adv Model Earth Syst 13:e2020MS002353
Whittleston D, Nicholson SE, Schlosser A, Entekhabi D (2017) Climate models lack jet-rainfall coupling over West Africa. J Clim 30:4625–4632. https://doi.org/10.1175/JCLI-D-16-0579.1
Worou K, Goosse H, Fichefet T et al (2020) Interannual variability of rainfall in the Guinean Coast region and its links with sea surface temperature changes over the twentieth century for the different seasons. Clim Dyn 55:449–470. https://doi.org/10.1007/s00382-020-05276-5
Worou K, Goosse H, Fichefet T, Kucharski F (2022) Weakened impact of the Atlantic Niño on the future equatorial Atlantic and Guinea Coast rainfall. Earth Syst Dyn 13:231–249. https://doi.org/10.5194/esd-13-231-2022
Wyser K, van Noije T, Yang S et al (2020) On the increased climate sensitivity in the EC-Earth model from CMIP5 to CMIP6. Geosci Model Dev 13:3465–3474. https://doi.org/10.5194/gmd-13-3465-2020
Xie S-P, Philander SGH (1994) A coupled ocean-atmosphere model of relevance to the ITCZ in the eastern Pacific. Tellus A 46:340–350. https://doi.org/10.1034/j.1600-0870.1994.t01-1-00001.x
Yukimoto S, Kawai H, Koshiro T et al (2019) The meteorological research institute earth system model version 2.0, MRI-ESM2.0: description and basic evaluation of the physical component. J Meteorol Soc Japan Ser II 97:931–965. https://doi.org/10.2151/jmsj.2019-051
Zappa G, Shepherd TG (2017) Storylines of atmospheric circulation change for European regional climate impact assessment. J Clim 30:6561–6577. https://doi.org/10.1175/JCLI-D-16-0807.1
Ziehn T, Chamberlain MA, Law RM et al (2020) The Australian earth system model: ACCESS-ESM1.5. J South Hemisph Earth Syst Sci. https://doi.org/10.1071/ES19035